Karlsruher Institut für Technologie

Kern- und Teilchenphysik

SS2012

Vorlesung-Website

- Johannes Blümer

KIT-Centrum Elementarteilchen- und Astroteilchenphysik KCETA

v20 3. Juli 2012 Neutrino-Oszillationen und -Masse

- Schwache Wechselwirkung
  - ...
  - Neutrinoquellen im Universum
  - Neutrino-Oszillationen
    - solare...
    - Reaktor...
    - atmosphärische...
    - Beschreibung
  - absolute Neutrinomasse
    - Dirac- oder Majorana-Masse?
    - Betazerfall
    - 0νßß-Zerfall
    - andere Methoden
- Von W- und Z-Bosonen zum Standardmodell

Erinnerung an v19

heute

Neutrinoquellen

[Georg Raffelt]

✔ Kernreaktoren


Sonne ✔

✔ Beschleuniger
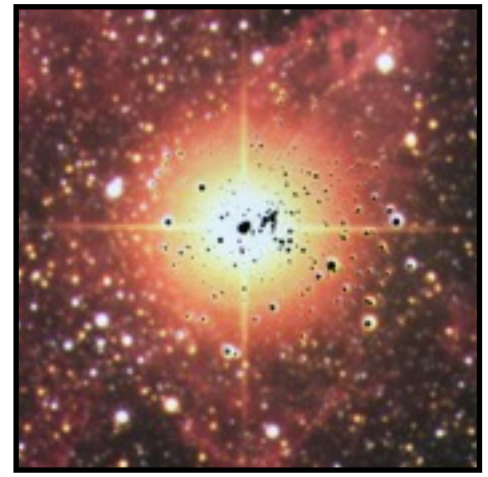
Supernovae ✔ 1987a

✔ Luftschauer
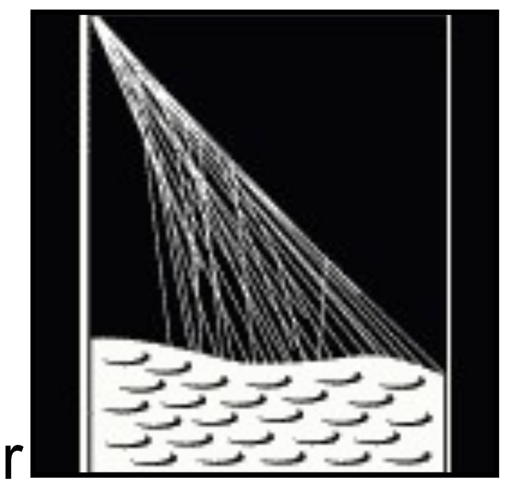
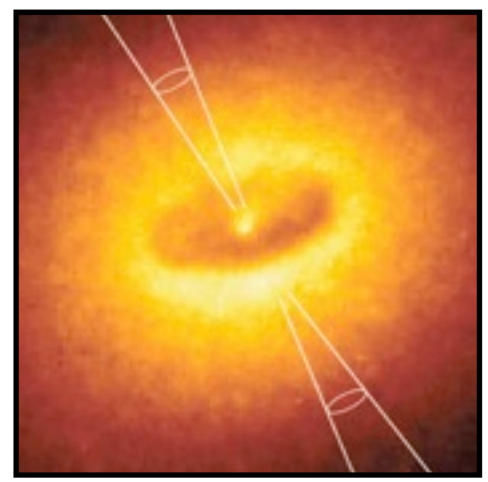
kosmische Beschleuniger ? noch nicht

gerade so ✔ Erdkruste


Urknall ✔ indirekt

Das Solare Neutrino-Problem und die Lösung

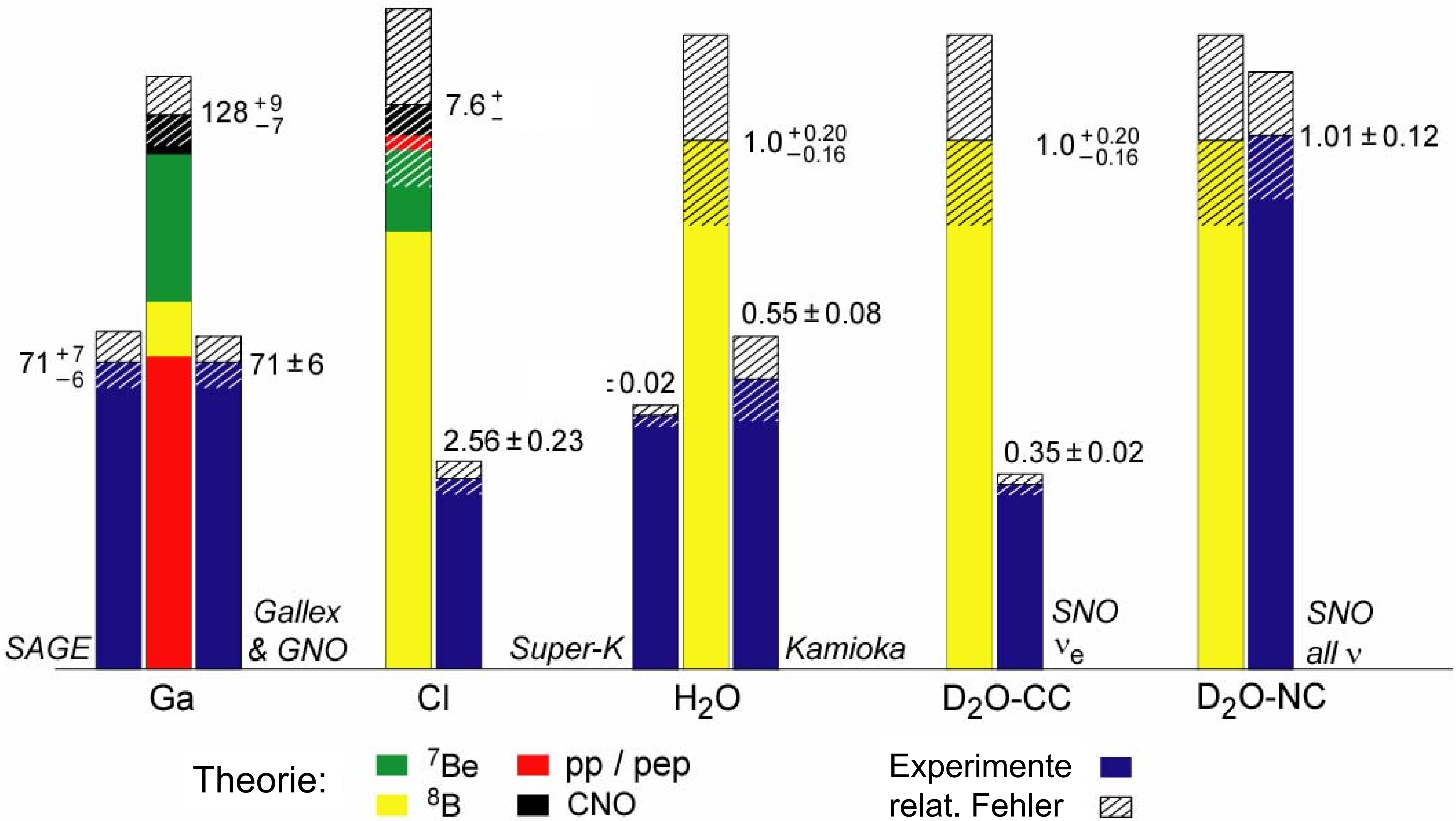

Neutrino-Oszillationen

QM-Betrachtung von ν-Oszillationen: Boris Kayser, hep-ph/0104147, 16 Apr2001

ν–Quelle

Flavourzustand

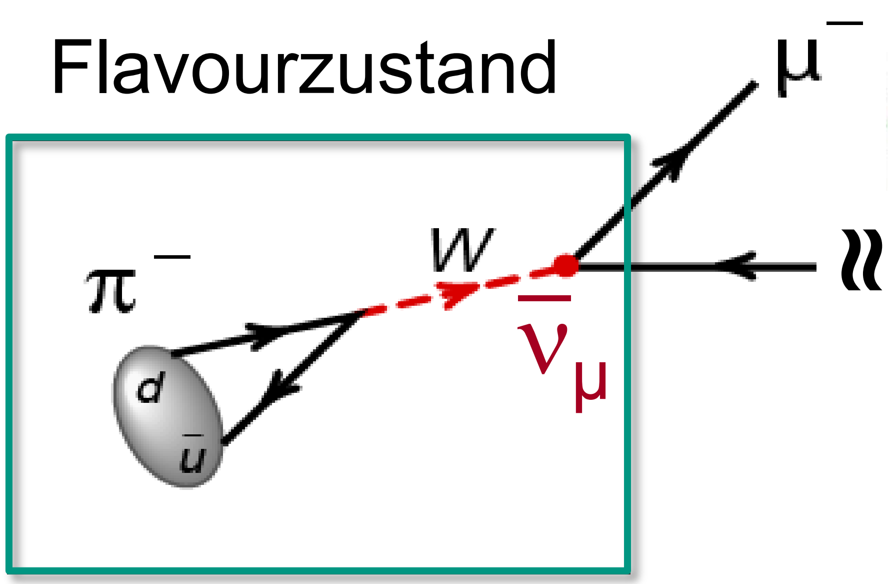

bei der Quelle muss bekannt sein:

ν–Energien
ν–Flüsse
ν–Arten

ν–Oszillationen

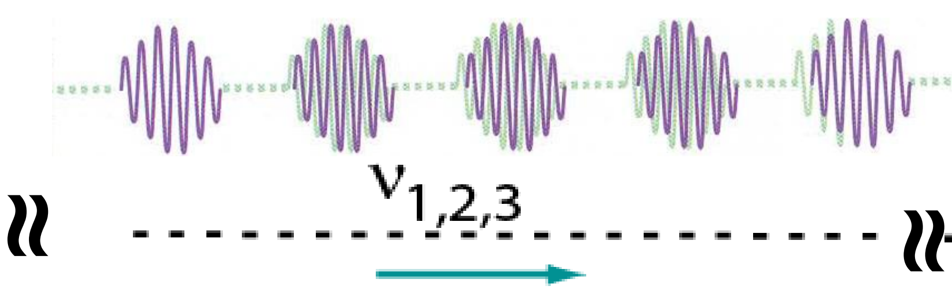

Propagation der ν–Massenzustände

L = 10 m … 10.000 km

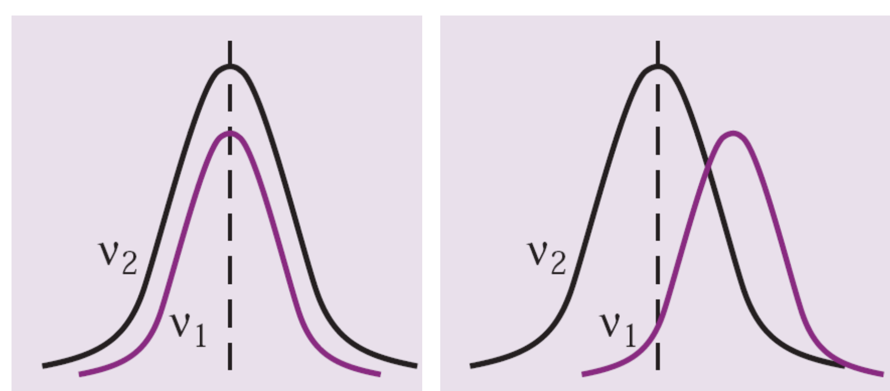

Emission Nachweis

ν–Nachweis

Flavourzustand

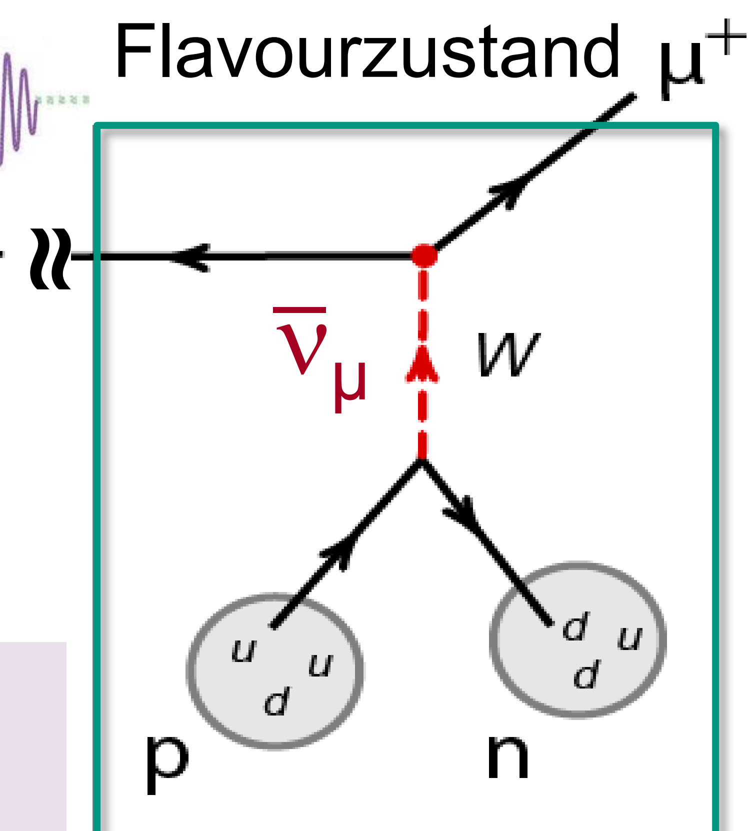

ν–Nachweiseffizienz
ν–Energieauflösung

[Drexlin]

Neutrino-Mischungsmatrix

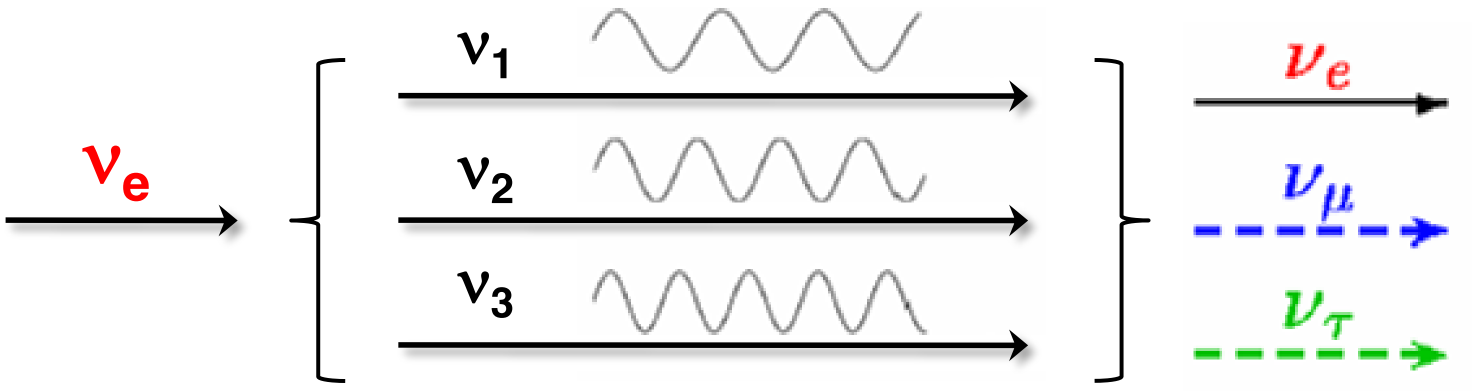

$\Delta m_{12}^2 = | m_1^2 - m_2^2 |$ 1. & 2. Generation

$\Delta m_{23}^2 = | m_2^2 - m_3^2 |$ 2. & 3. Generation

$\Delta m_{13}^2 = | m_1^2 - m_3^2 |$ 1. & 3. Generation

leptonische Mischungsmatrix:
Pontecorvo-Maki-Nakagawa-Sakata

$$\begin{pmatrix} \nu_e \\ \nu_\mu \\ \nu_\tau \end{pmatrix} = \begin{pmatrix} U_{e1} & U_{e2} & U_{e3} \\ U_{\mu 1} & U_{\mu 2} & U_{\mu 3} \\ U_{\tau 1} & U_{\tau 2} & U_{\tau 3} \end{pmatrix} \cdot \begin{pmatrix} \nu_1 \\ \nu_2 \\ \nu_3 \end{pmatrix}$$

U = unitäre 3 × 3 Mischungsmatrix

Oszillationsmuster

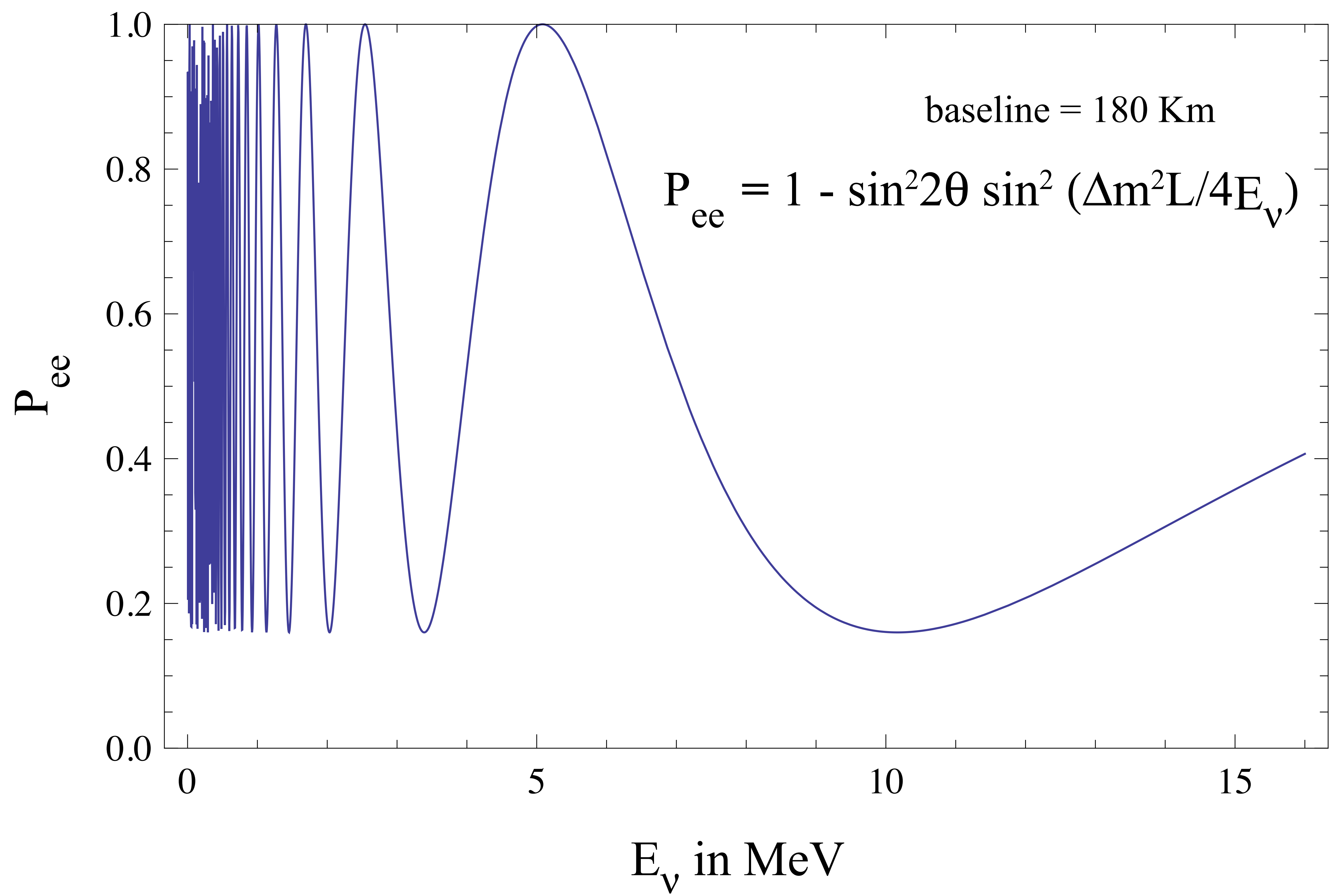

Figure 13.1: The ν_e ($\bar{\nu}_e$) survival probability $P(\nu_e \rightarrow \nu_e) = P(\bar{\nu}_e \rightarrow \bar{\nu}_e)$, Eq. (13.30), as a function of the neutrino energy for $L = 180$ km, $\Delta m^2 = 7.0 \times 10^{-5}$ eV^2 and $\sin^2 2\theta = 0.84$ (from Ref. 62). [RPP]

Table 13.1: Sensitivity of different oscillation experiments.

Source	Type of ν	$\overline{E}$[MeV]	L[km]	$\min(\Delta m^2)$[eV^2]
Reactor	$\overline{\nu}_e$	~ 1	1	$\sim 10^{-3}$
Reactor	$\overline{\nu}_e$	~ 1	100	$\sim 10^{-5}$
Accelerator	$\nu_\mu, \overline{\nu}_\mu$	$\sim 10^3$	1	~ 1
Accelerator	$\nu_\mu, \overline{\nu}_\mu$	$\sim 10^3$	1000	$\sim 10^{-3}$
Atmospheric ν's	$\nu_{\mu,e}, \overline{\nu}_{\mu,e}$	$\sim 10^3$	10^4	$\sim 10^{-4}$
Sun	ν_e	~ 1	1.5×10^8	$\sim 10^{-11}$

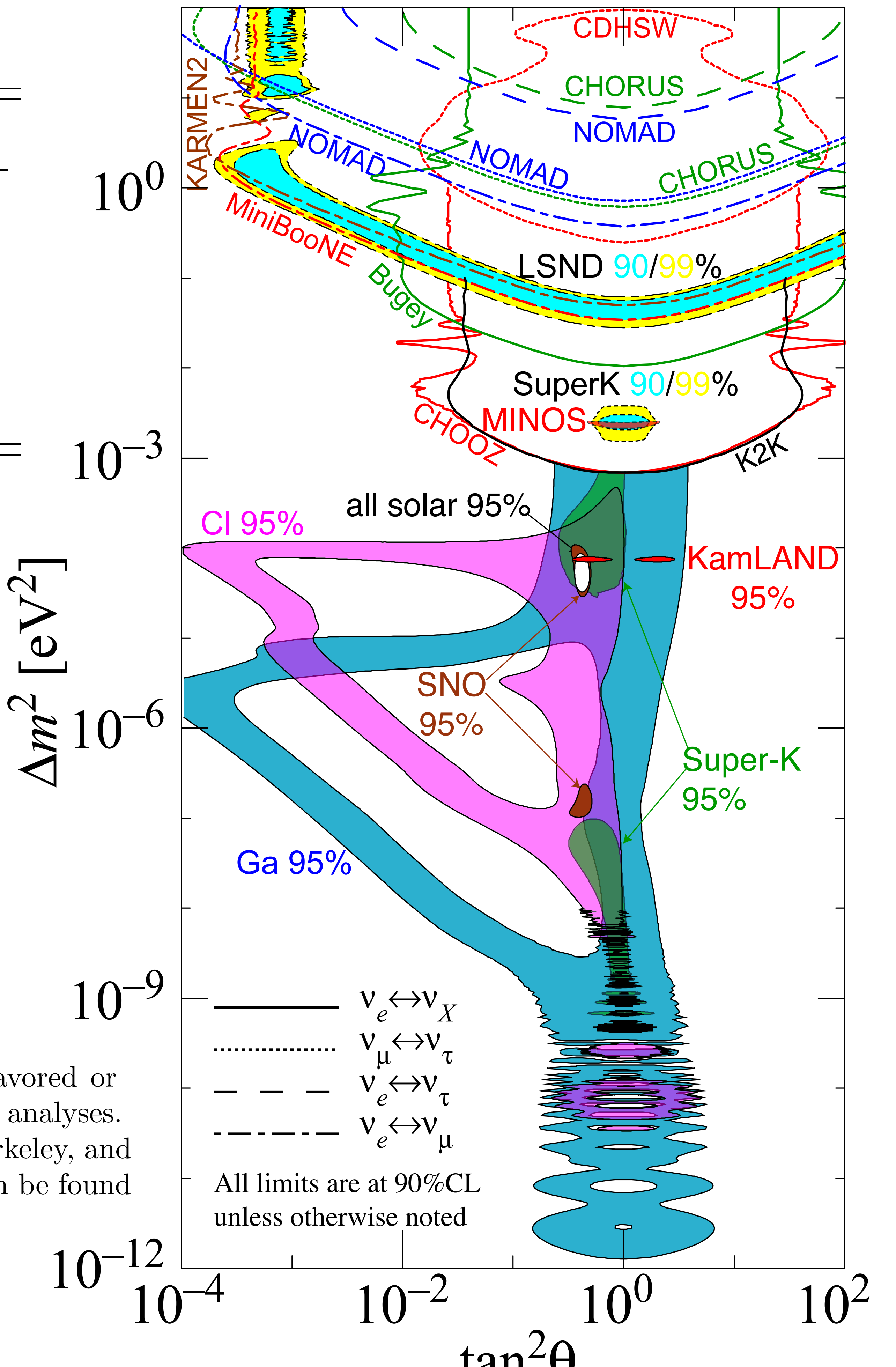

Figure 13.9: The regions of squared-mass splitting and mixing angle favored or excluded by various experiments based on two-flavor neutrino oscillation analyses. The figure was contributed by H. Murayama (University of California, Berkeley, and IPMU, University of Tokyo). References to the data used in the figure can be found at `http://hitoshi.berkeley.edu/neutrino`.

[RPP]

KamLand

KAMioka Liquid scintillator Anti-Neutrino Detector

KamLAND is at the site of the former Kamiokande experiment at a depth of $\sim$2700 m water equivalent. The heart of the detector is 1 kton of highly purified liquid scintillator (LS) enclosed in an EVOH/nylon balloon suspended in purified mineral oil. The LS consists of 80% dodecane, 20% pseudocumene and 1.36 ± 0.03 g/l of PPO [4]. The anti-neutrino detector is inside an 18-m-diameter stainless steel sphere. An array of 1879 50-cm-diameter photomultiplier tubes (PMTs) is mounted on the inner surface of the sphere. 554 of these are reused from the Kamiokande experiment, while the remaining 1325 are a faster version masked to 17 inches. A 3.2-kton cylindrical water-Cherenkov outer detector (OD), surrounding the containment sphere, provides shielding and operates as an active cosmic-ray veto detector.

Electron anti-neutrinos are detected via inverse β-decay, $\overline{\nu}_e + p \to e^+ + n$, with a 1.8 MeV threshold. The prompt scintillation light from the e^+ gives a measure of the $\overline{\nu}_e$ energy, $E_{\overline{\nu}_e} \simeq E_\mathrm{p} + \overline{E}_n + 0.8\,\mathrm{MeV}$, where E_p is the prompt event energy including the positron kinetic and annihilation energy, and $\overline{E}_n$ is the average neutron recoil energy, O(10 keV). The mean neutron capture time is $207.5 \pm 2.8\,\mu$s. More than 99% capture on free protons, producing a 2.2 MeV γ ray.

KamLAND is surrounded by 55 Japanese nuclear power reactor units, each an isotropic $\overline{\nu}_e$ source. The reactor operation records, including thermal power generation, fuel burnup, and exchange and enrichment logs, are provided by a consortium of Japanese electric power companies. This information, combined with publicly available world reactor data, is used to calculate the instantaneous fission rates using a reactor model [5]. Only four isotopes contribute significantly to the $\overline{\nu}_e$ spectra; the ratios of the fission yields averaged over the entire data taking period are: $^{235}\mathrm{U} : {}^{238}\mathrm{U} : {}^{239}\mathrm{Pu} : {}^{241}\mathrm{Pu} = 0.570 : 0.078 : 0.295 : 0.057$. The emitted $\overline{\nu}_e$ energy spectrum is calculated using the $\overline{\nu}_e$ spectra inferred from Ref. [6], while the spectral uncertainty is evaluated from Ref. [7]. We also include contributions from the long-lived fission daughters ^{90}Sr, ^{106}Ru, and ^{144}Ce [8].

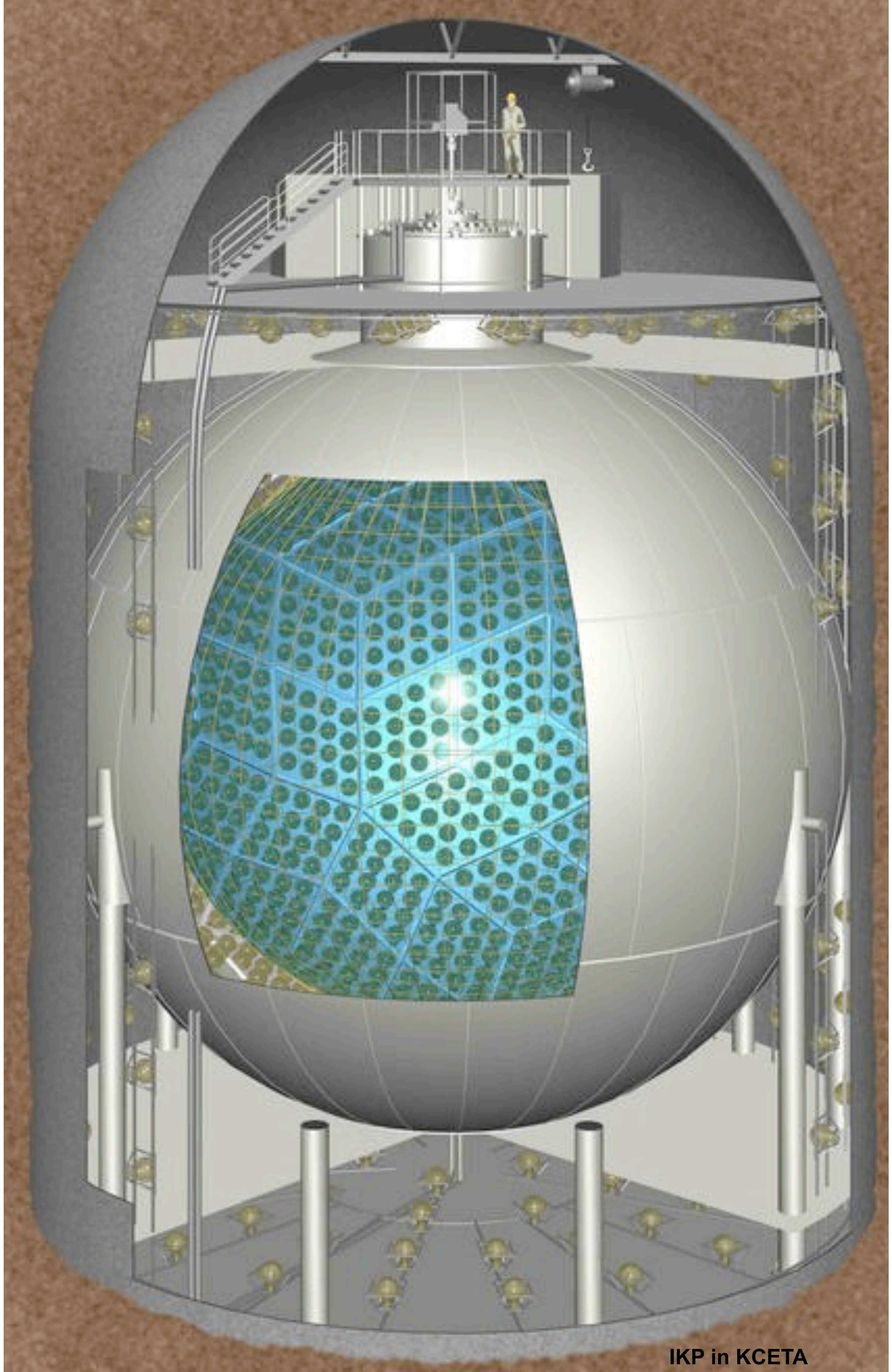

[Kamland web]

Kamland Daten: ν_e-Verschwinden

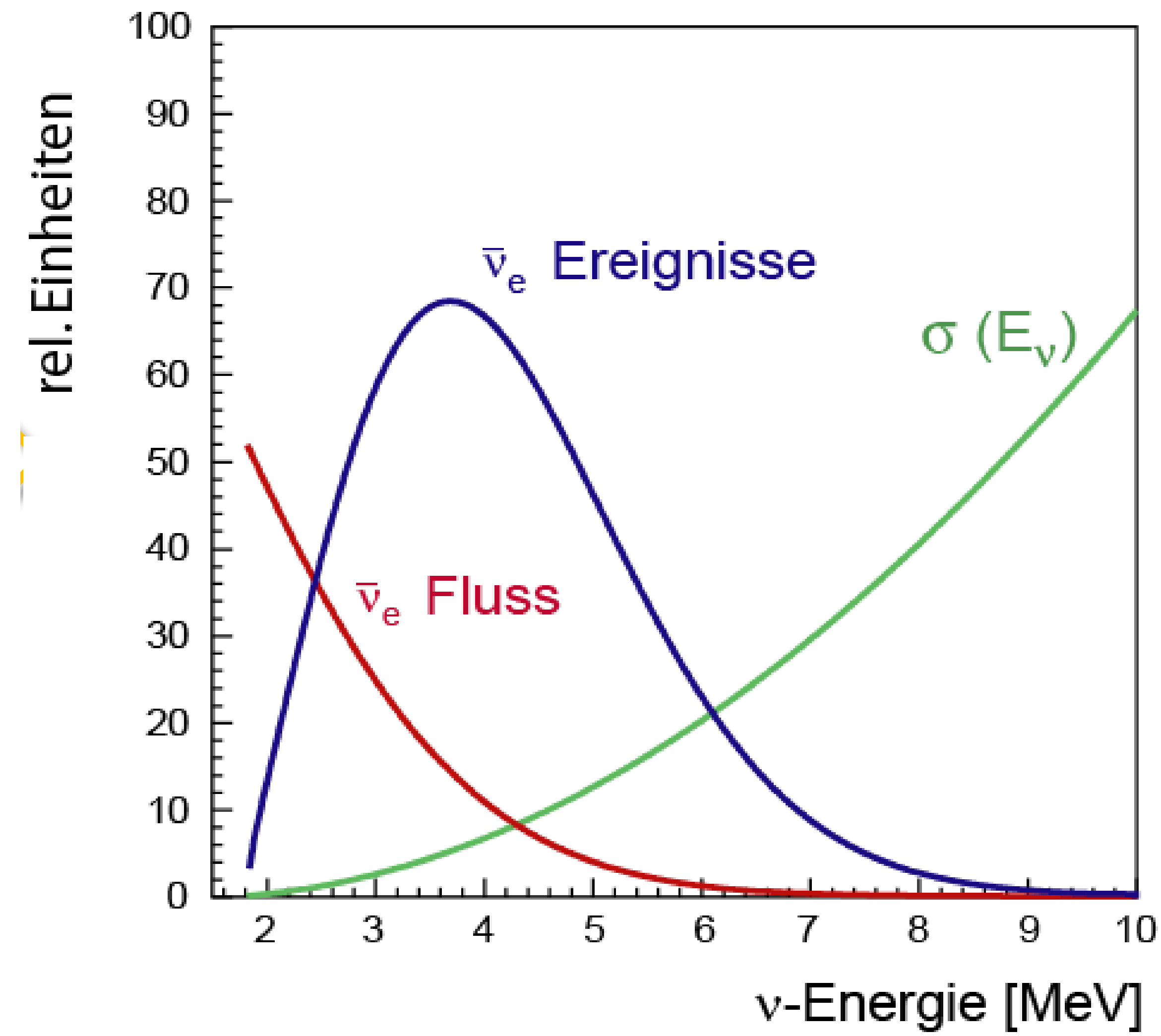

Erinnerung an die zu erwartenden Energiespektren von Neutrinos aus Spaltreaktionen...

Kamland Daten: ν_e-Verschwinden

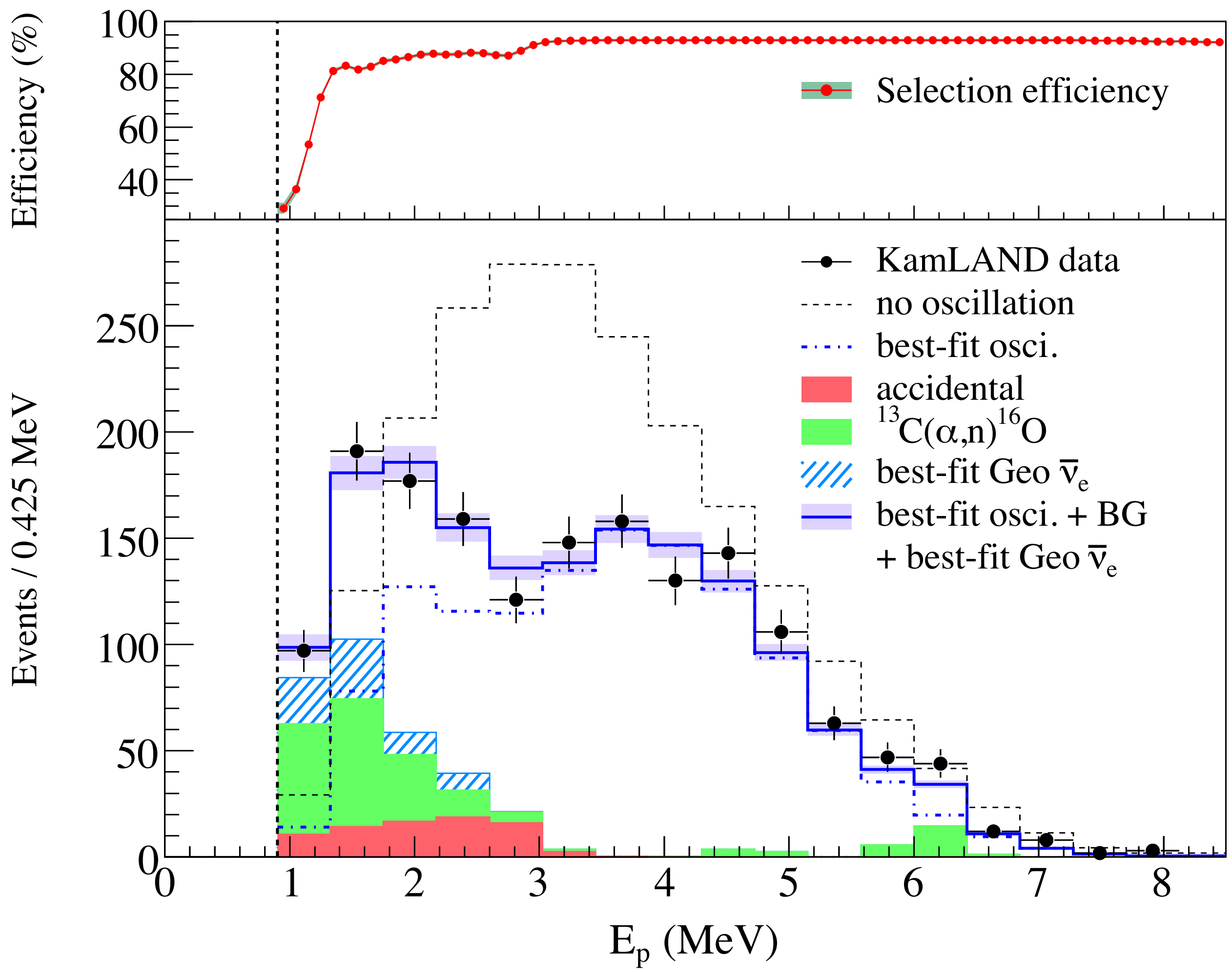

FIG. 1: Prompt event energy spectrum of $\overline{\nu}_e$ candidate events. All histograms corresponding to reactor spectra and expected backgrounds incorporate the energy-dependent selection efficiency (top panel). The shaded background and geo-neutrino histograms are cumulative. Statistical uncertainties are shown for the data; the band on the blue histogram indicates the event rate systematic uncertainty.

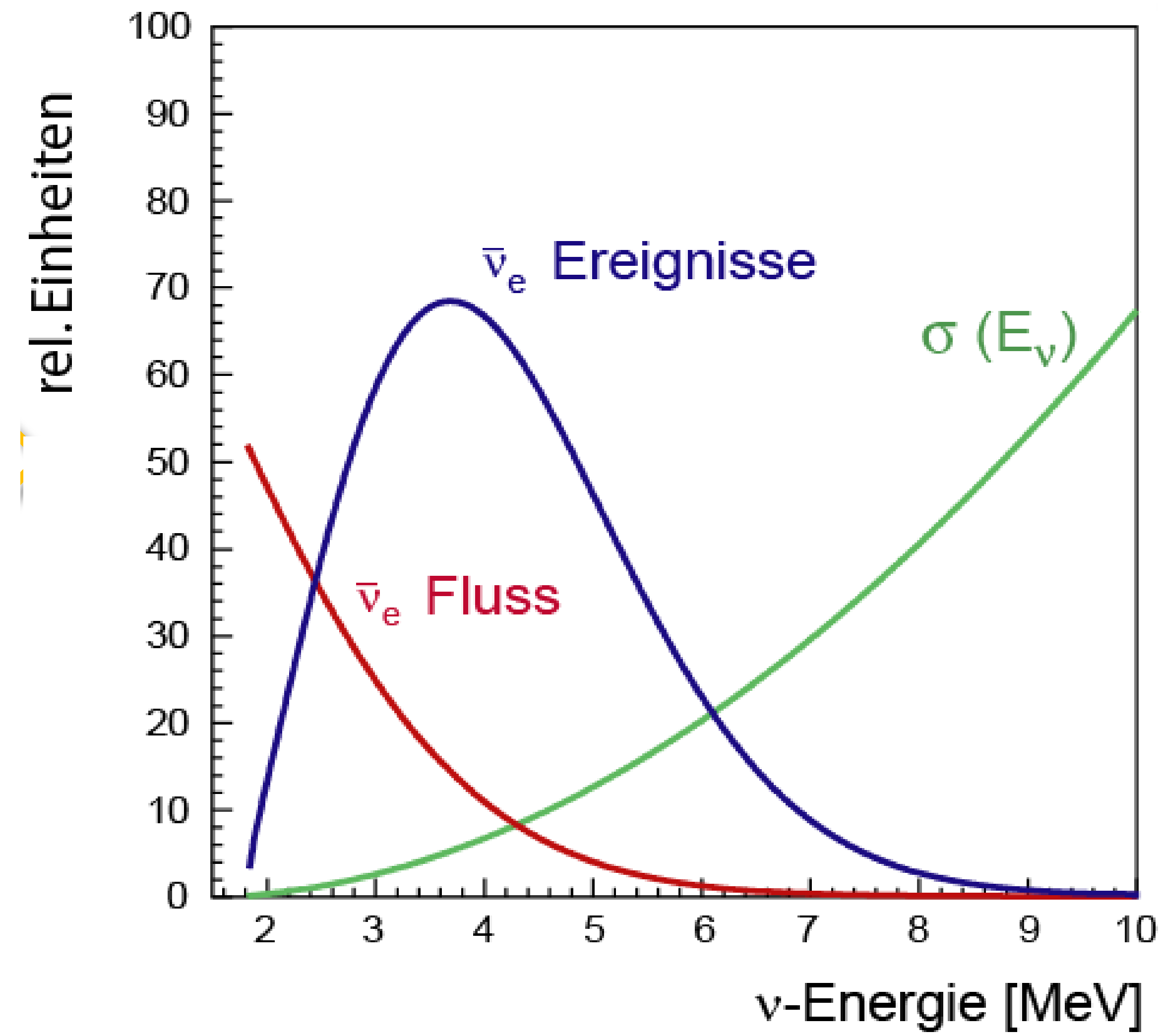

Erinnerung an die zu erwartenden Energiespektren von Neutrinos aus Spaltreaktionen...

Kamland Daten: ν_e-Verschwinden

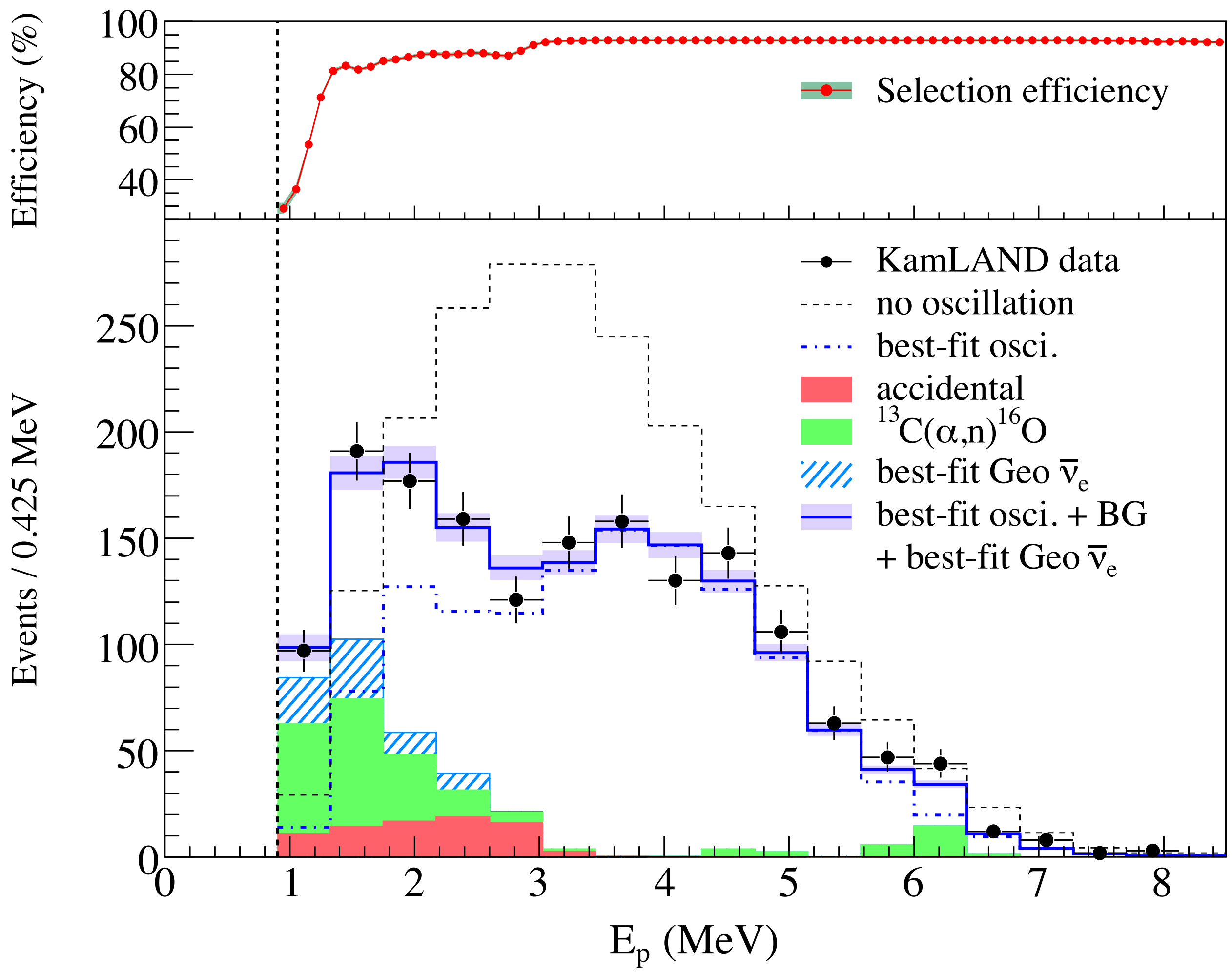

FIG. 1: Prompt event energy spectrum of $\overline{\nu}_e$ candidate events. All histograms corresponding to reactor spectra and expected backgrounds incorporate the energy-dependent selection efficiency (top panel). The shaded background and geo-neutrino histograms are cumulative. Statistical uncertainties are shown for the data; the band on the blue histogram indicates the event rate systematic uncertainty.

Phys. Rev. Lett. 100, 221803 (2008)

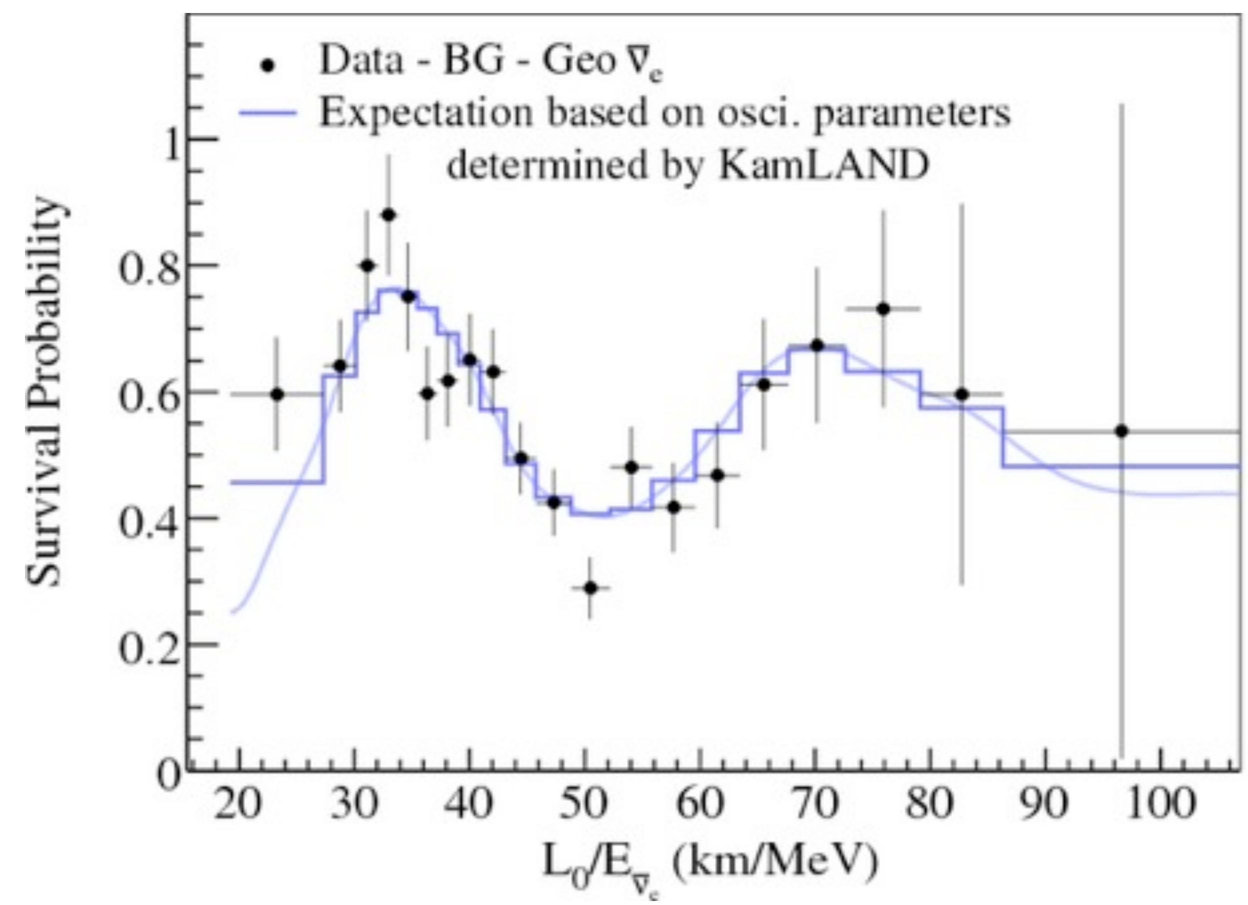

Ratio of the background and geo-neutrino subtracted anti-neutrino spectrum to the expectation for no-oscillation as a function of L/E. L is the effective baseline taken as a flux-weighted average (L=180km). The histogram and curve show the expectation accounting for the distances to the individual reactors, time-dependent flux variations and efficiencies. The figure shows the behavior expected from neutrino oscillation, where the electron anti-neutrino survival probability is:

$$P_{ee} = 1 - sin^2 2\theta sin^2(\Delta m^2 \frac{L}{E})$$

Atmosphärische Neutrinos

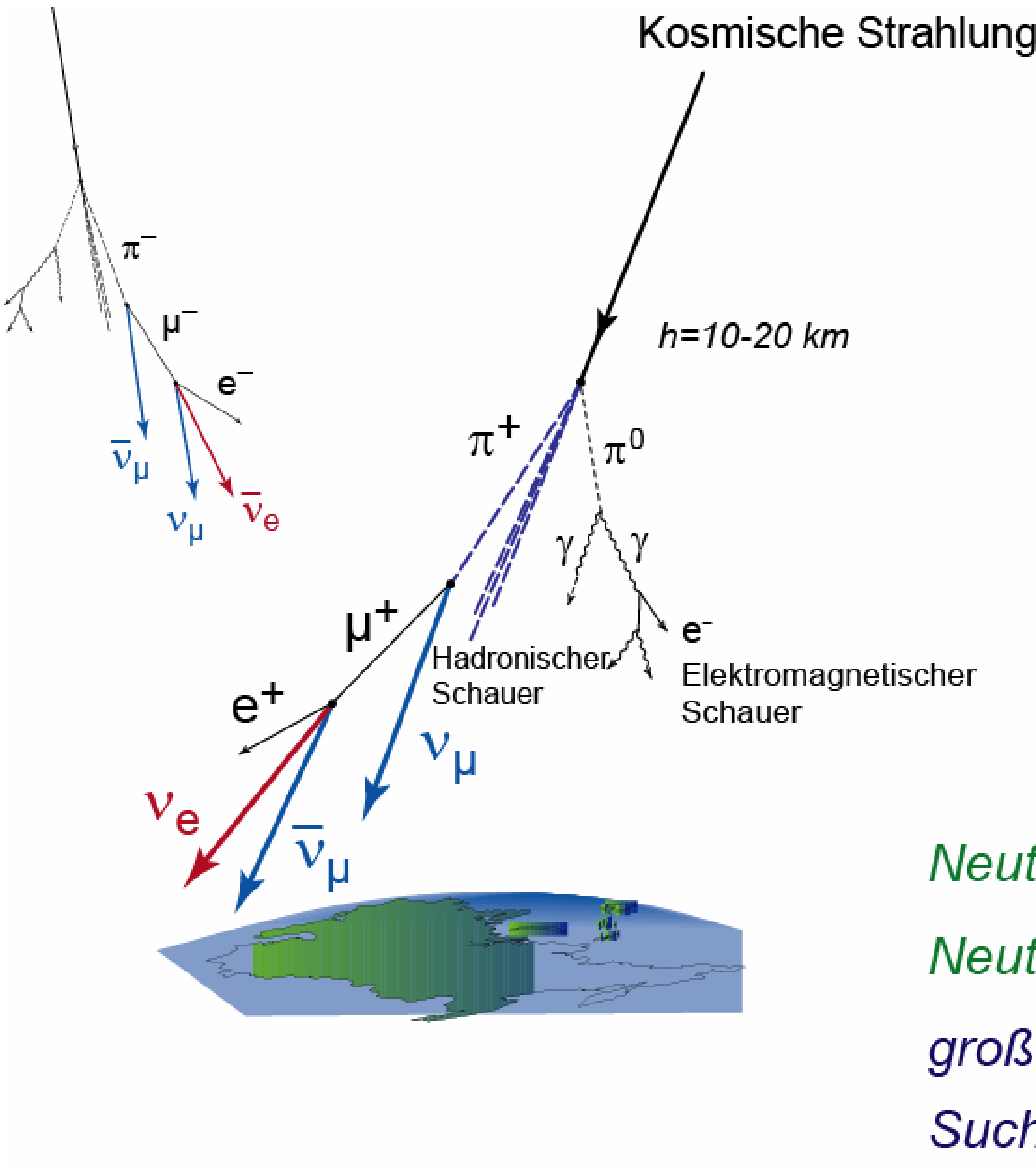

$$\pi^+ \rightarrow \mu^+ + \nu_\mu$$
(p,He,..)
$$\hookrightarrow e^+ + \nu_e + \bar{\nu}_\mu$$

weiterhin: π^- μ^- e^- Zerfallskette
Kaonenzerfälle K^+, K^-

Flavour-Verhätlnis $\nu_\mu : \nu_e = 2 : 1$

für breiten Energiebereich: E_ν = 1-20 GeV!

geomagnetische Effekte für E_ν < 2 GeV !

Neutrino-Energien: E_ν = 0.5 - 500 GeV

Neutrino-Flugstrecke: L_ν = 12 - 12.000 km

große L/E Variation, auch kleine Δm^2 - Werte

Suche nach ν_μ - ν_e and ν_μ - ν_τ Oszillationen

Super-Kamiokande

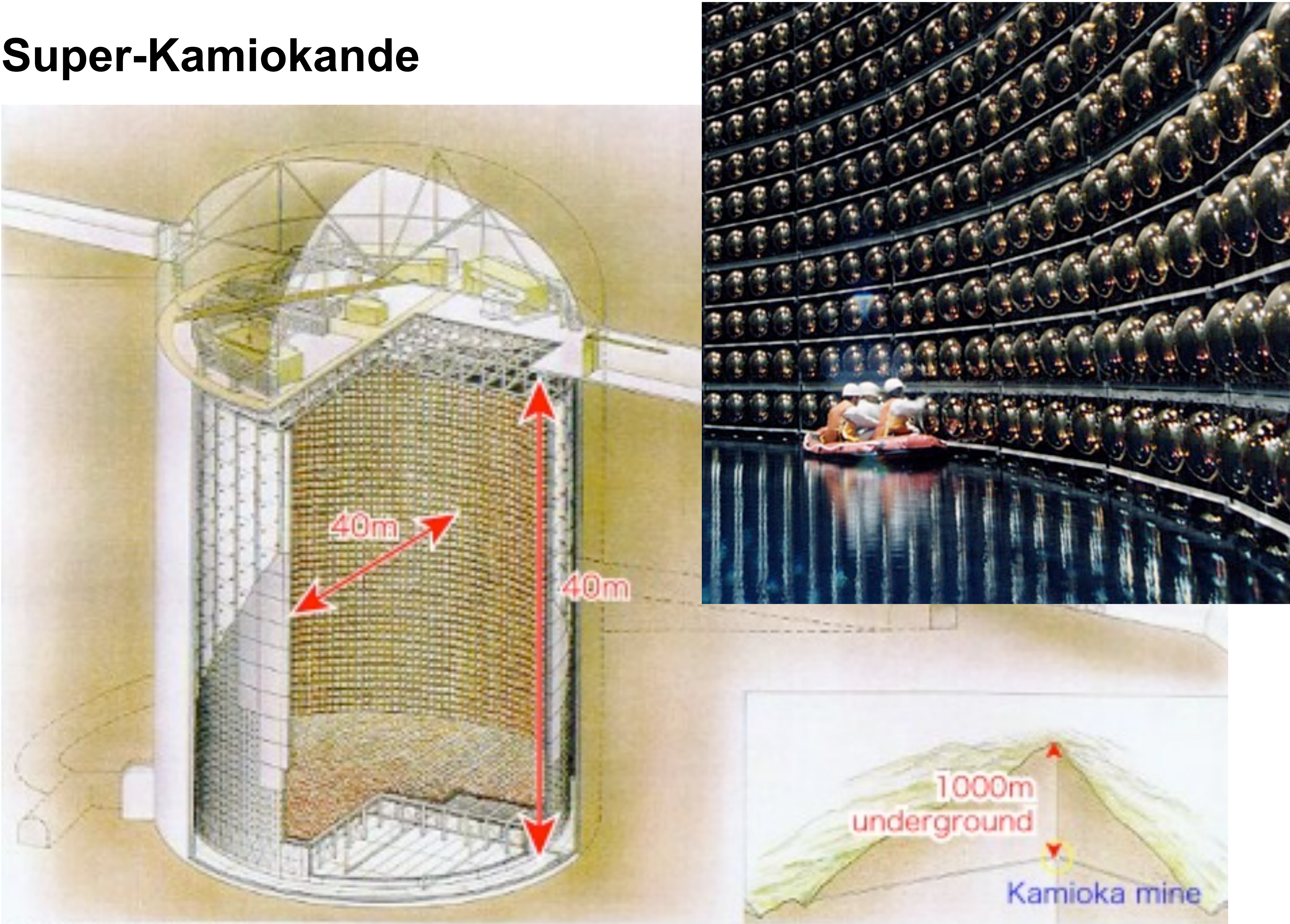

SUPER-KAMIOKANDE

The New York Times

VOL. CXLVII .... No. 51,179

NEW YORK, FRIDAY, JUNE 5, 1998

$1 beyond the greater New York metropolitan area.

Mass Found in Elusive Particle; Universe May Never Be the Same

Discovery on Neutrino Rattles Basic Theory About All Matter

By MALCOLM W. BROWNE

TAKAYAMA, Japan, June 5 — In what colleagues hailed as a historic landmark, 120 physicists from 23 research institutions in Japan and the United States announced today that they had found the existence of mass in a notoriously elusive subatomic particle called the neutrino.

The neutrino, a particle that carries no electric charge, is so light that it was assumed for many years to have no mass at all. After today's announcement, cosmologists will have to confront the possibility that a significant part of the mass of the universe might be in the form of neutrinos. The discovery will also compel scientists to revise a highly successful theory of the composition of matter known as the Standard Model.

Word of the discovery had drawn some 300 physicists here to discuss neutrino research. Among other things, the finding of neutrino mass might affect theories about the formation and evolution of galaxies and the ultimate fate of the universe. If neutrinos have sufficient mass, their presence throughout the universe would increase the overall mass of

Detecting Neutrinos

And Detecting Their Mass

By analyzing the cones of light, physicists determine that some neutrinos have changed form on their journey. If they can change form, they must have mass.

Scientists Find Mass in an Elusive Particle, Rattling a Basic Theory About All Matter

But once in a great while, a neutrino does hit an atom and the resulting blast of nuclear debris supplies clues about the neutrino itself. The debris generally includes many particles that can race through water, mineral oil or even ice, sending out shock waves of blue light. This light, called Cherenkov radiation, can be detected by sensitive light sensors and measured.

During the past few decades, scientists have learned that matter is made up of three distinct flavors or types. This means that there are three flavors of neutrinos — the electron neutrino associated with the electron, the muon neutrinos, associated with the muon particle, which is a kind of fat electron, and the tau neutrino, associated with the tau particle, an even fatter relative of the electron. The role of the muon and tau particles and their associated neutrinos in the universe has mystified physicists. "Who ordered that?" the Columbia University physicist Isidor Rabi is said to have remarked when the muon was found.

The Super-Kamiokande detector was built two years ago as a joint Japanese-American experiment. It is essentially a water tank the size of a large cathedral installed in a deep zinc mine one mile inside a mountain 30 miles north of here. When neutrinos slice through the tank, one of them occasionally makes its presence known by colliding with an

yet been directly detected but it must exist to make observations consistent.)

A related problem has to do with neutrinos produced by the fusion process in the sun. This process, which merges the nuclei of hydrogen atoms to form helium nuclei and energy, produces neutrinos. Astro physicists believe they understand the mechanism in complete detail.

The trouble is that all the best detectors ever built find far fewer neutrinos than should be present according to understanding of the fusion reaction.

Scientists believe the anomaly can be explained by the oscillation of detectable solar nutrinos into types that cannot be detected by existing instruments. But no one has proved this explanation.

Worldwide Efforts To Unlock Secrets

Members of the Kamiokande collaboration have not limited their in-

(The electron-volt is used by scientists as a unit of particle mass. One electron-volt is the energy, or mass equivalent, that an electron acquires by passing through an electric potential of one volt. By this standard a neutrino is believed to have a mass only about five-hundred-thousandth as much as that of an electron, which itself is a light particle.)

In the last 68 years, a legion of distinguished physicists has devoted inquiries and careers to the puzzling neutrino, which was given its name by the great Italian-American scientist Enrico Fermi. Fermi quickly came to believe in the particle's existence, even though it was not proved in his lifetime, and named it "neutrino," which means "little neutral one" in Italian.

Representatives of dozens of neutrino experiments meet once every two years to exchange ideas at conferences like the one under way here. Present are representatives of teams that have installed neutrino detectors on the bottom of Lake Baikal in Siberia, under the Aegean Sea

e/μ-Identifizierung in Super-Kamiokande

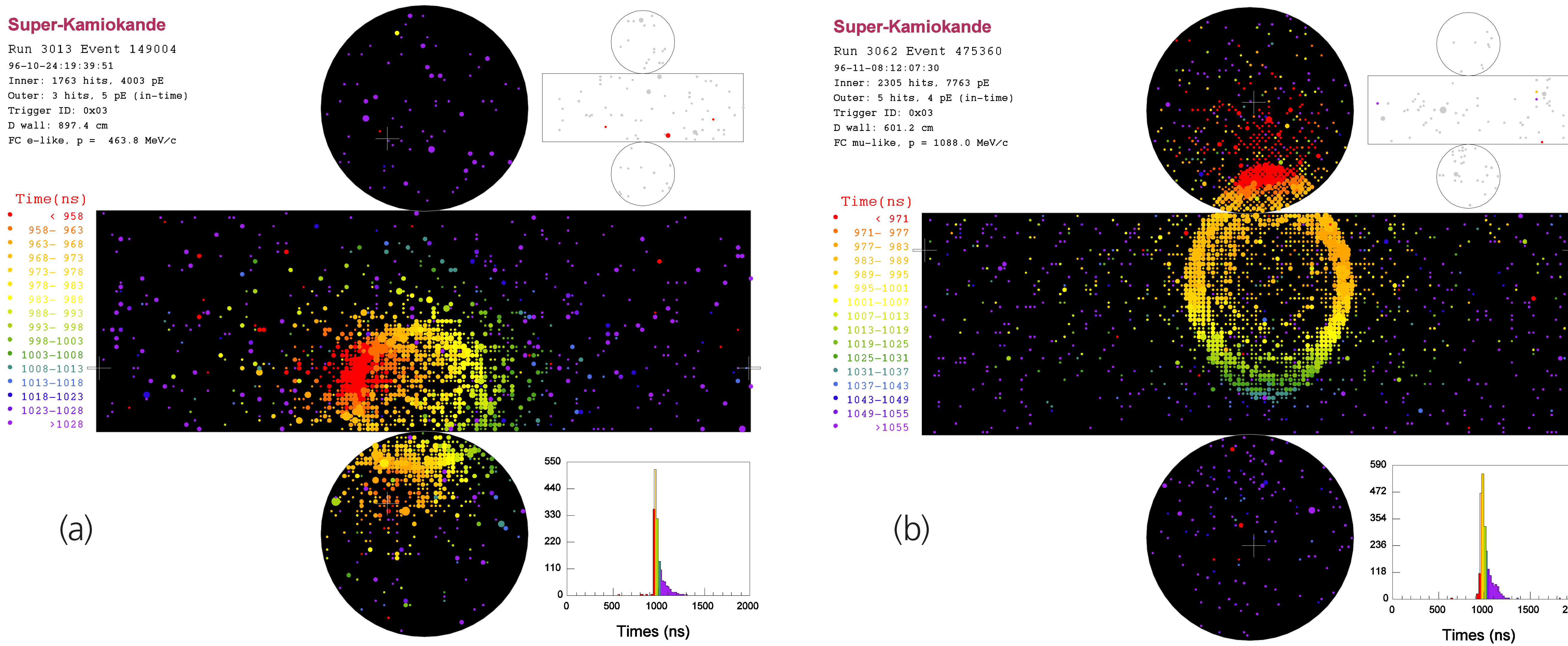

Figure 2. Examples of (a) electron neutrino and (b) muon neutrino events observed in Super-Kamiokande. The sizes of the circles in this figure show the observed light intensity. Also, the color of the circles shows the timing information of the observed light.

[KAVLI IPMU Tokyo http://www.ipmu.jp/node/1148]

Super-K atm-ν

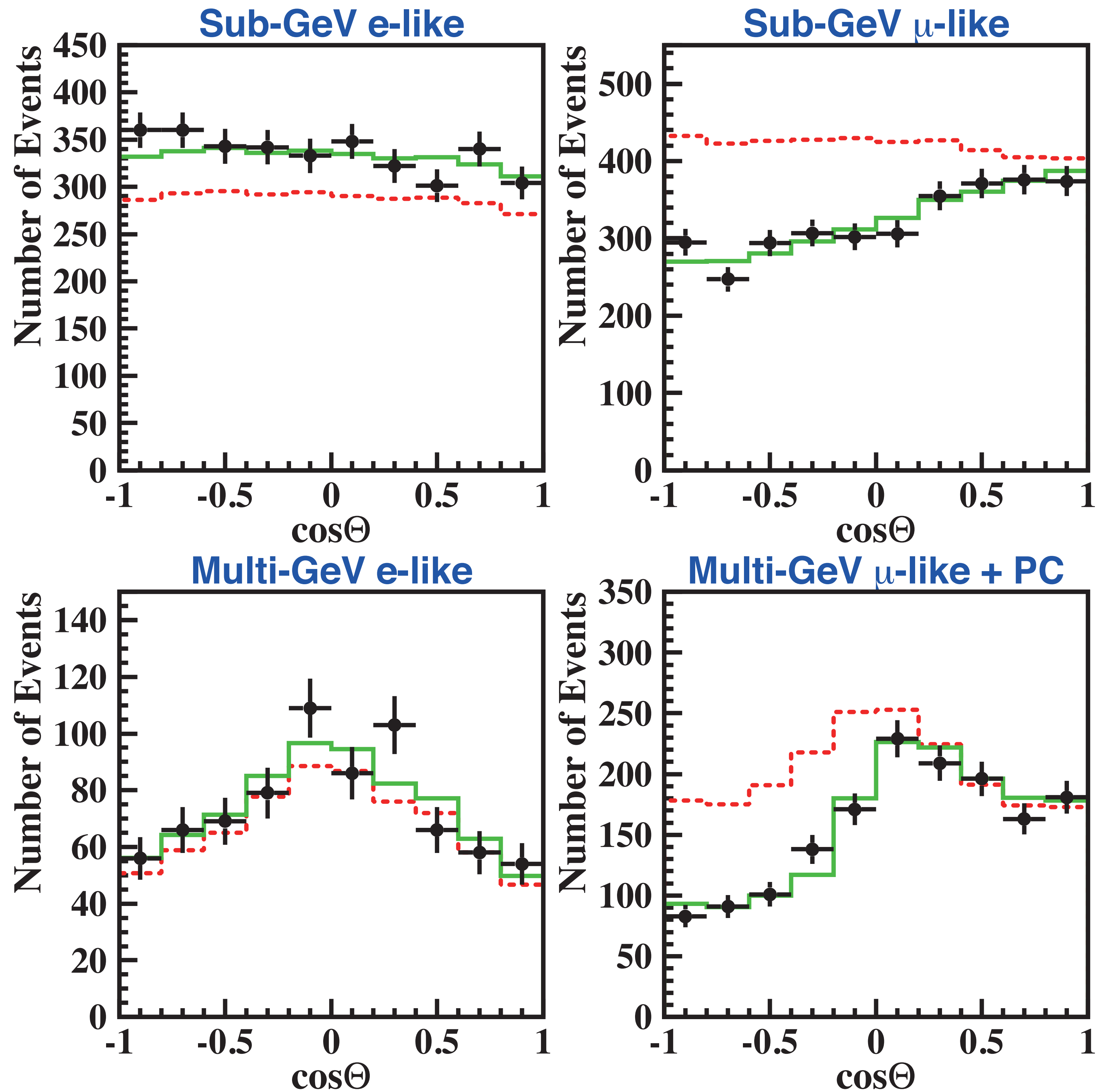

[RPP] **Figure 13.5:** The zenith angle distributions for fully contained 1-ring e-like and μ-like events with visible energy < 1.33 GeV (sub-GeV) and > 1.33 GeV (multi-GeV). For multi-GeV μ-like events, a combined distribution with partially contained (PC) events is shown. The dotted histograms show the non-oscillated Monte Carlo events, and the solid histograms show the best-fit expectations for $\nu_\mu \leftrightarrow \nu_\tau$ oscillations. (This figure is provided by the Super-Kamiokande Collab.)

Neutrino-Oszillationen Gesamtschau

$$U = \begin{pmatrix} 1 & 0 & 0 \\ 0 & \cos\theta_{23} & \sin\theta_{23} \\ 0 & -\sin\theta_{23} & \cos\theta_{23} \end{pmatrix} \cdot \begin{pmatrix} \cos\theta_{13} & 0 & \sin\theta_{13} e^{-i\delta} \\ 0 & 1 & 0 \\ -\sin\theta_{13} e^{-i\delta} & 0 & \cos\theta_{13} \end{pmatrix} \cdot \begin{pmatrix} \cos\theta_{12} & \sin\theta_{12} & 0 \\ -\sin\theta_{12} & \cos\theta_{12} & 0 \\ 0 & 0 & 1 \end{pmatrix}$$

δ: CP-Phase

2. & 3. Generation	1. & 3. Generation	1. & 2. Generation
atmosphärische ν´s	Reaktorexperimente	solare Neutrinos
long baseline Beschleuniger	long baseline Beschleuniger	Reaktorexperimente
ν_μ - X, ν_μ - ν_τ	$\bar{\nu}_e$ – X, ν_μ - ν_e	ν_e - X, $\bar{\nu}_e$ – X
$\Delta m_{23}^2 = 2.3 \times 10^{-3}$ eV²	$\Delta m_{13}^2 = 2.3 \times 10^{-3}$ eV²	$\Delta m_{12}^2 = 7.9 \times 10^{-5}$ eV²
$\theta_{23} = (45 \pm 4)°$ (maximal)	$\theta_{13} < 15°$ (sehr klein)	$\theta_{23} = (33.7 \pm 1.3)°$ (groß)

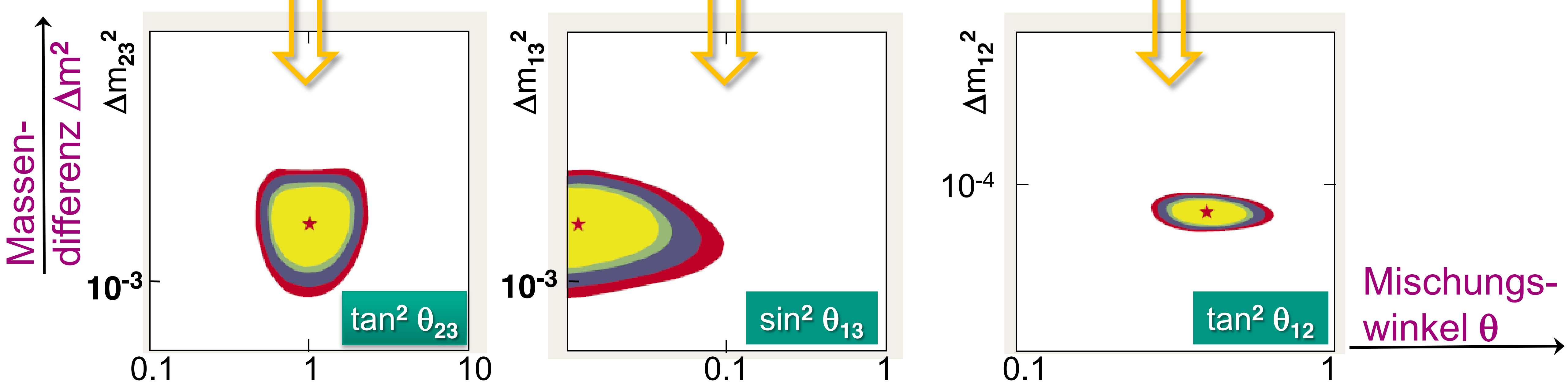

[Drexlin 2010, siehe update]

Theta-13

The $\overline{\nu}_e$ is detected via the inverse β-decay (IBD) reaction, $\overline{\nu}_e + p \rightarrow e^+ + n$, in a Gadolinium-doped liquid scintillator (Gd-LS) [9, 10]. The coincidence of the prompt scintillation from the e^+ and the delayed neutron capture on Gd provides a distinctive $\overline{\nu}_e$ signature.

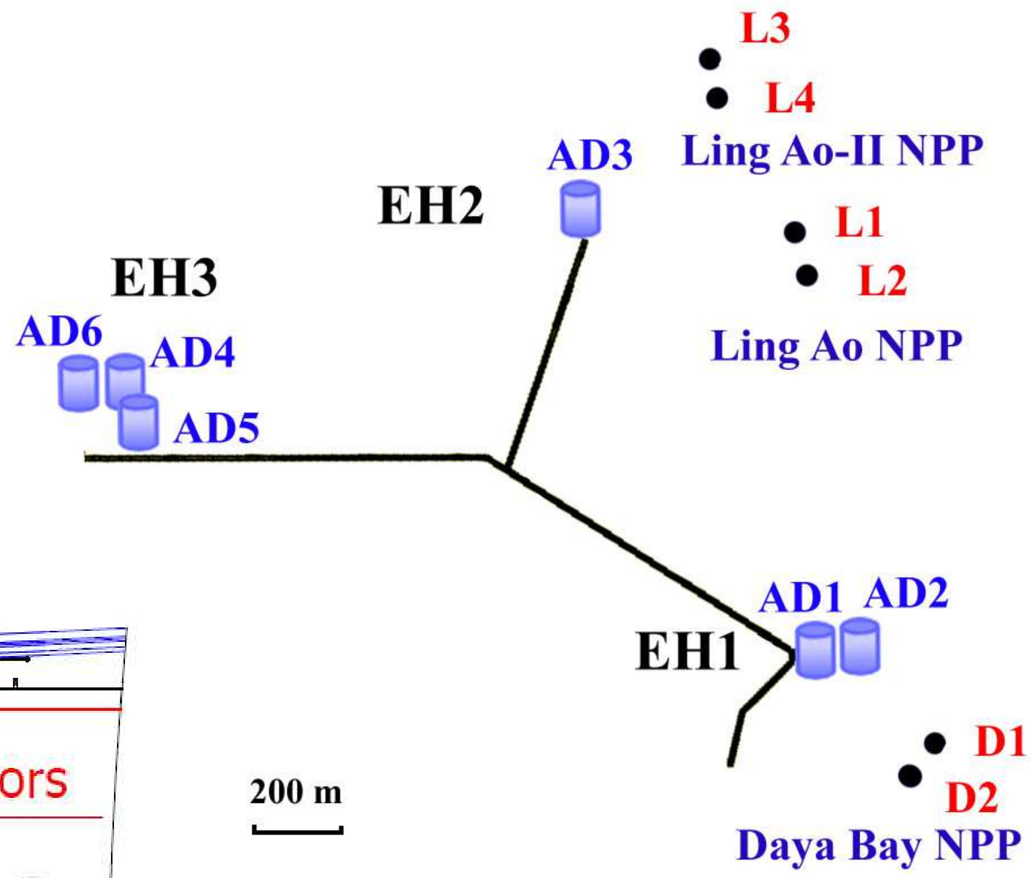

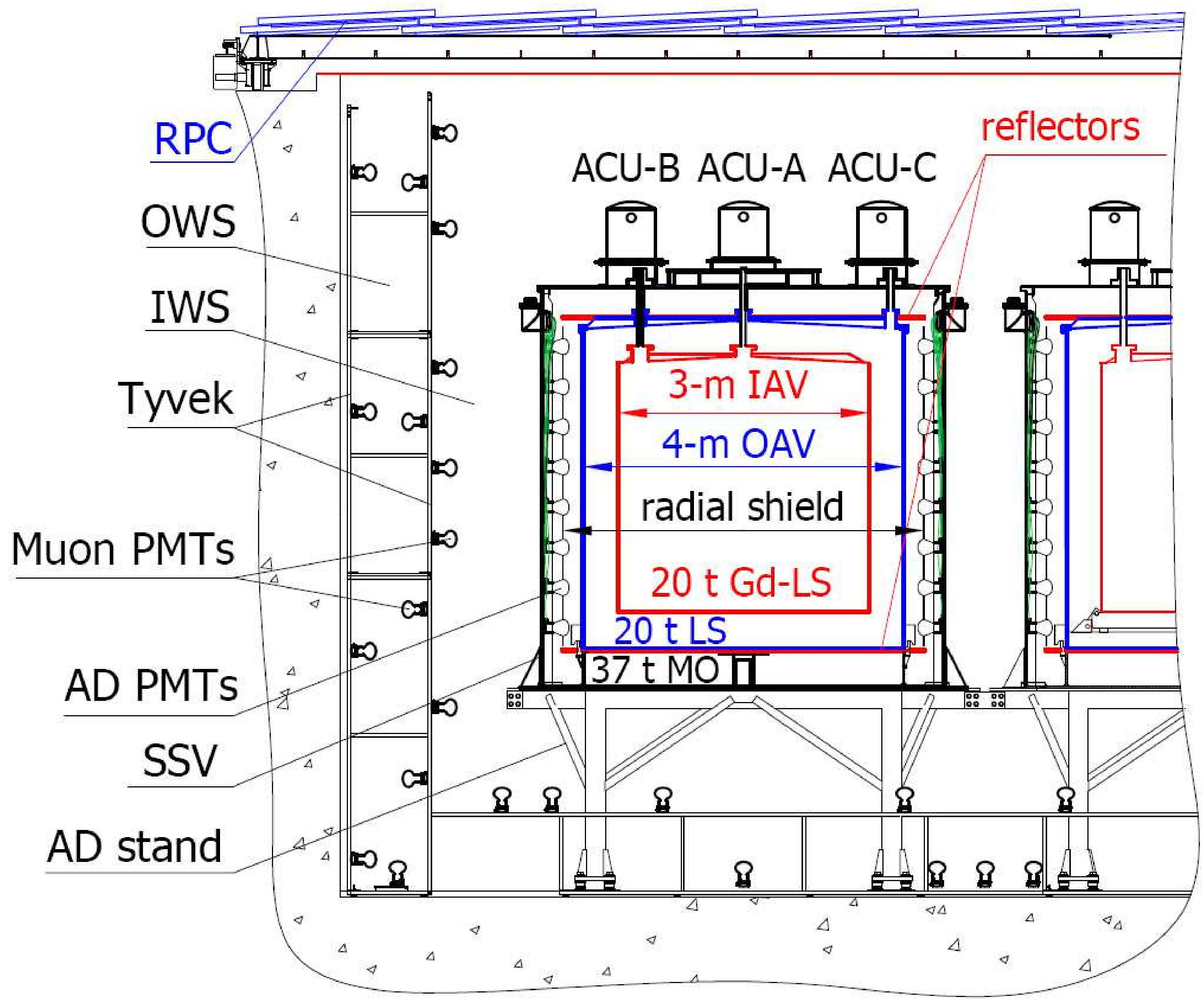

[Daya Bay arXiv: 1203.1669v2]

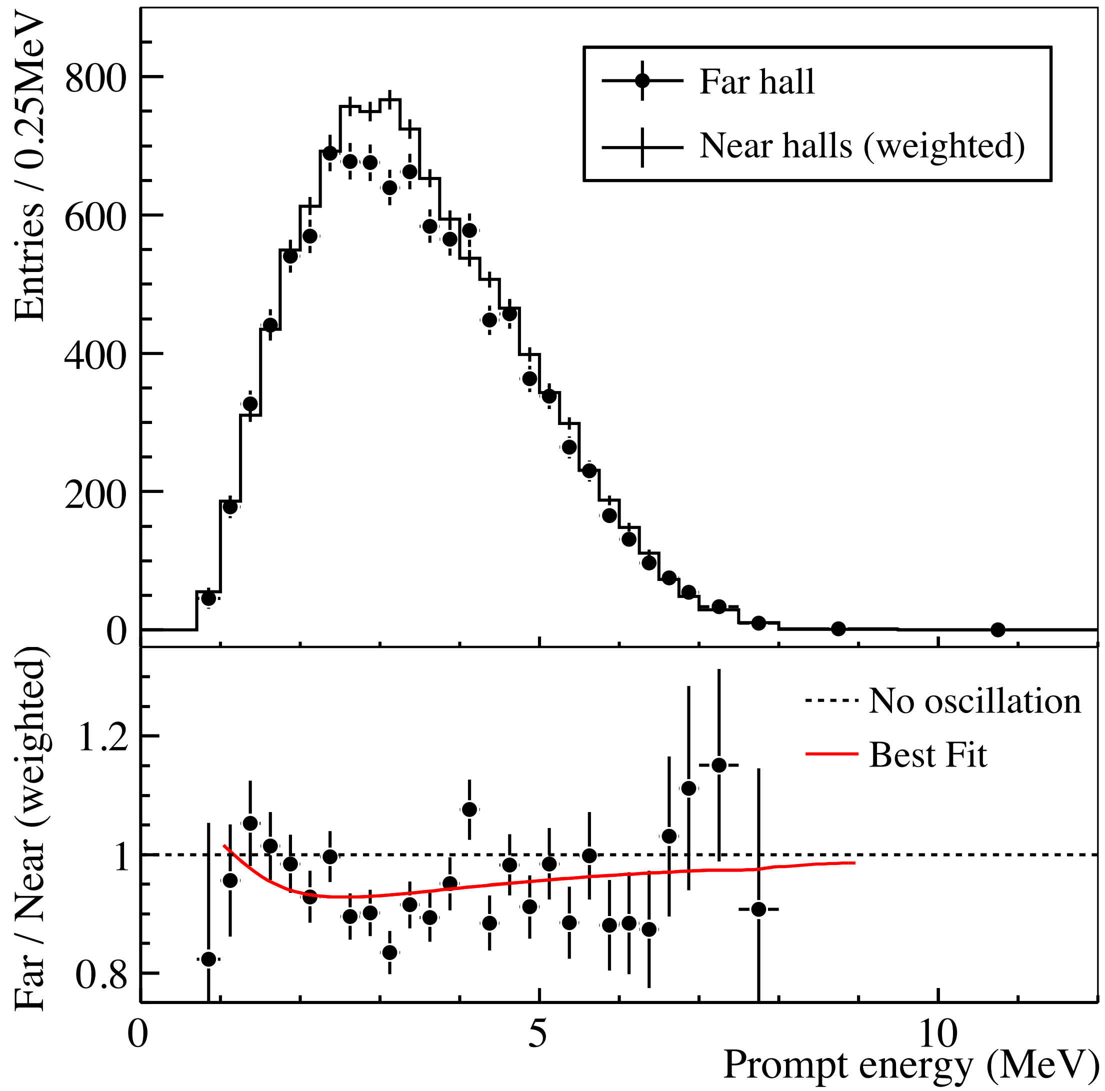

FIG. 5. Top: Measured prompt energy spectrum of the far hall (sum of three ADs) compared with the no-oscillation prediction from the measurements of the two near halls. Spectra were background subtracted. Uncertainties are statistical only. Bottom: The ratio of measured and predicted no-oscillation spectra. The red curve is the best-fit solution with $\sin^2 2\theta_{13} = 0.092$ obtained from the rate-only analysis. The dashed line is the no-oscillation prediction.

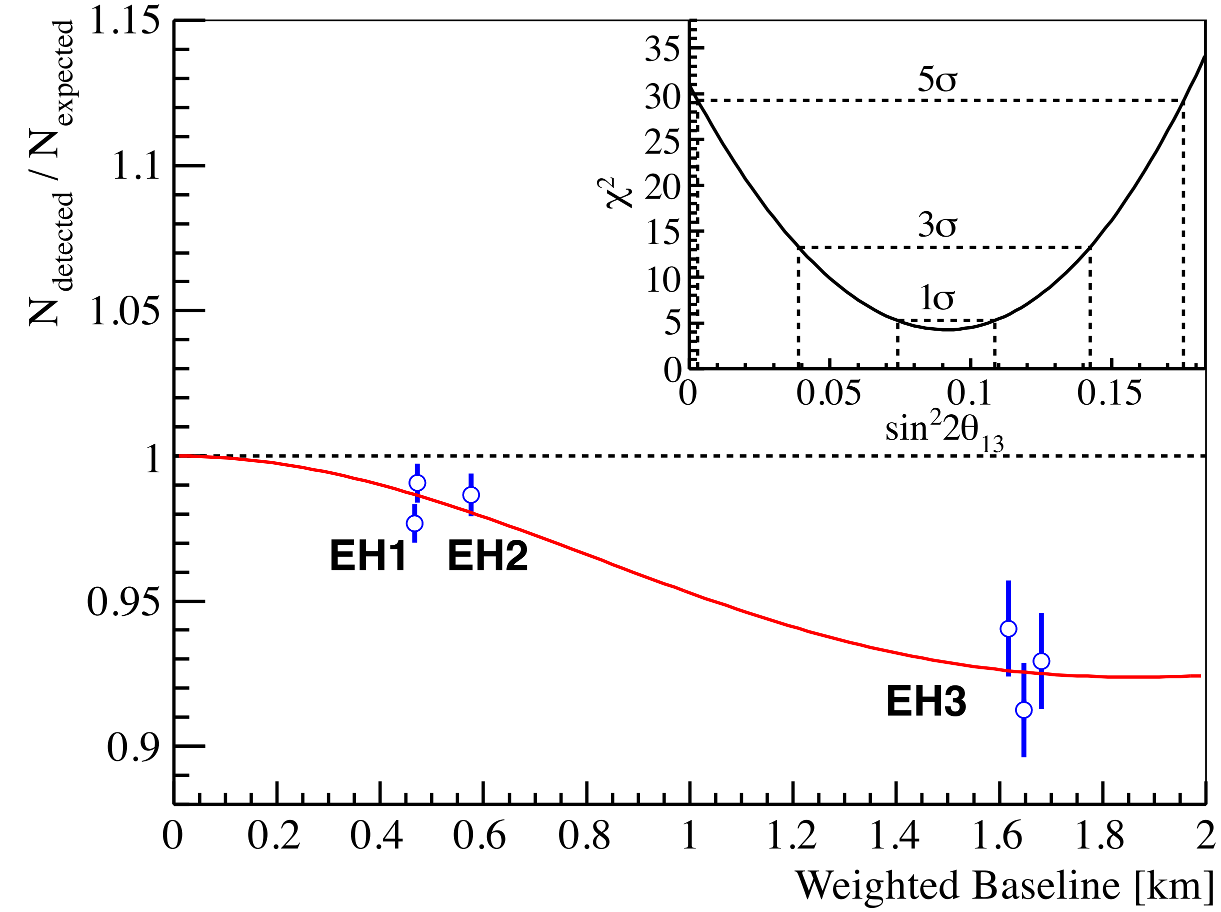

FIG. 4. Ratio of measured versus expected signal in each detector, assuming no oscillation. The error bar is the uncorrelated uncertainty of each AD, including statistical, detector-related, and background-related uncertainties. The expected signal is corrected with the best-fit normalization parameter. Reactor and survey data were used to compute the flux-weighted average baselines. The oscillation survival probability at the best-fit value is given by the smooth curve. The AD4 and AD6 data points are displaced by -30 and +30 m for visual clarity. The χ^2 versus $\sin^2 2\theta_{13}$ is shown in the inset.

$\sin^2 2\theta_{13} = 0.092 \pm 0.016(\text{stat}) \pm 0.005(\text{syst})$
in a three-neutrino framework.

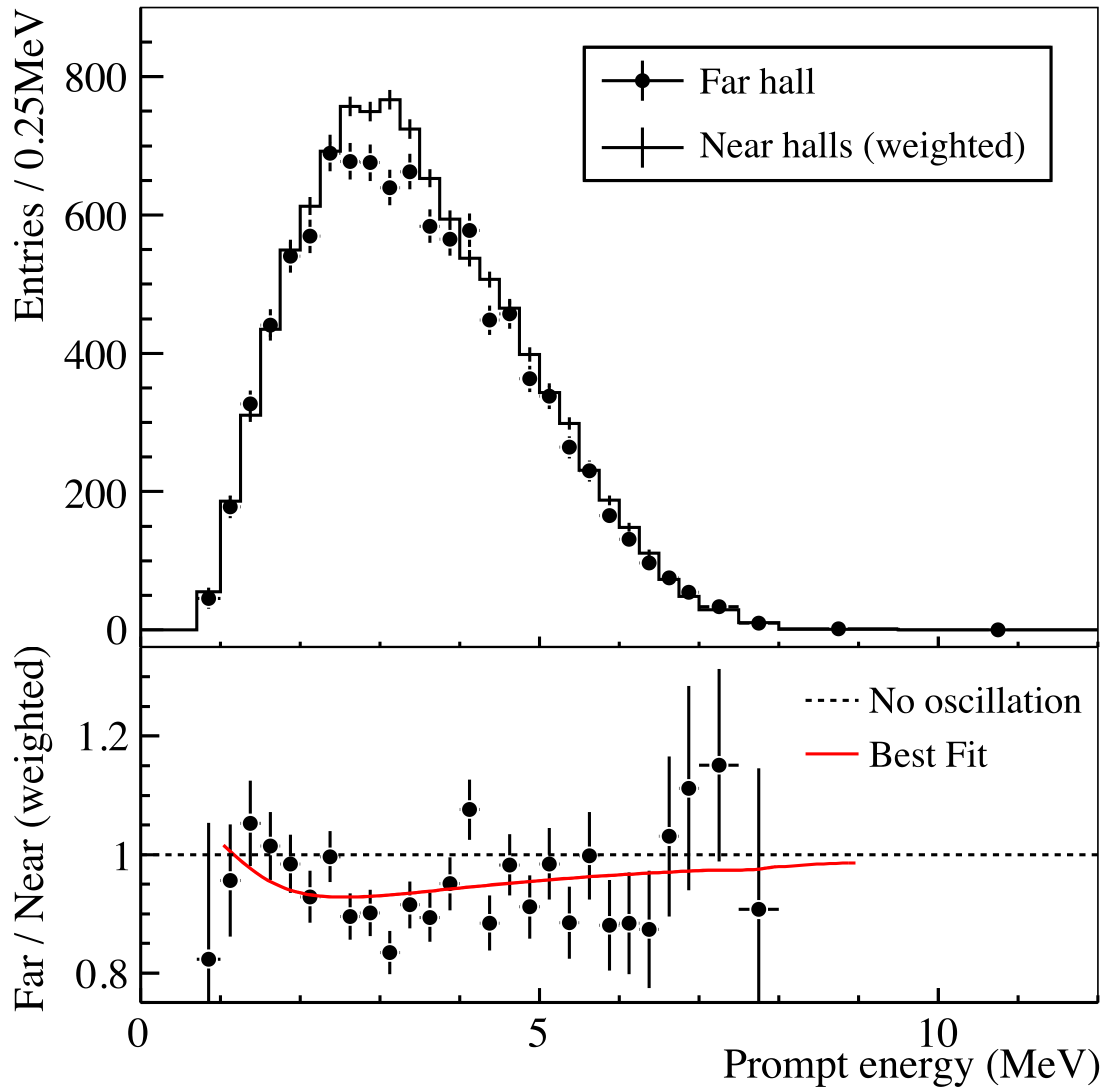

FIG. 5. Top: Measured prompt energy spectrum of the far hall (sum of three ADs) compared with the no-oscillation prediction from the measurements of the two near halls. Spectra were background subtracted. Uncertainties are statistical only. Bottom: The ratio of measured and predicted no-oscillation spectra. The red curve is the best-fit solution with $\sin^2 2\theta_{13} = 0.092$ obtained from the rate-only analysis. The dashed line is the no-oscillation prediction.

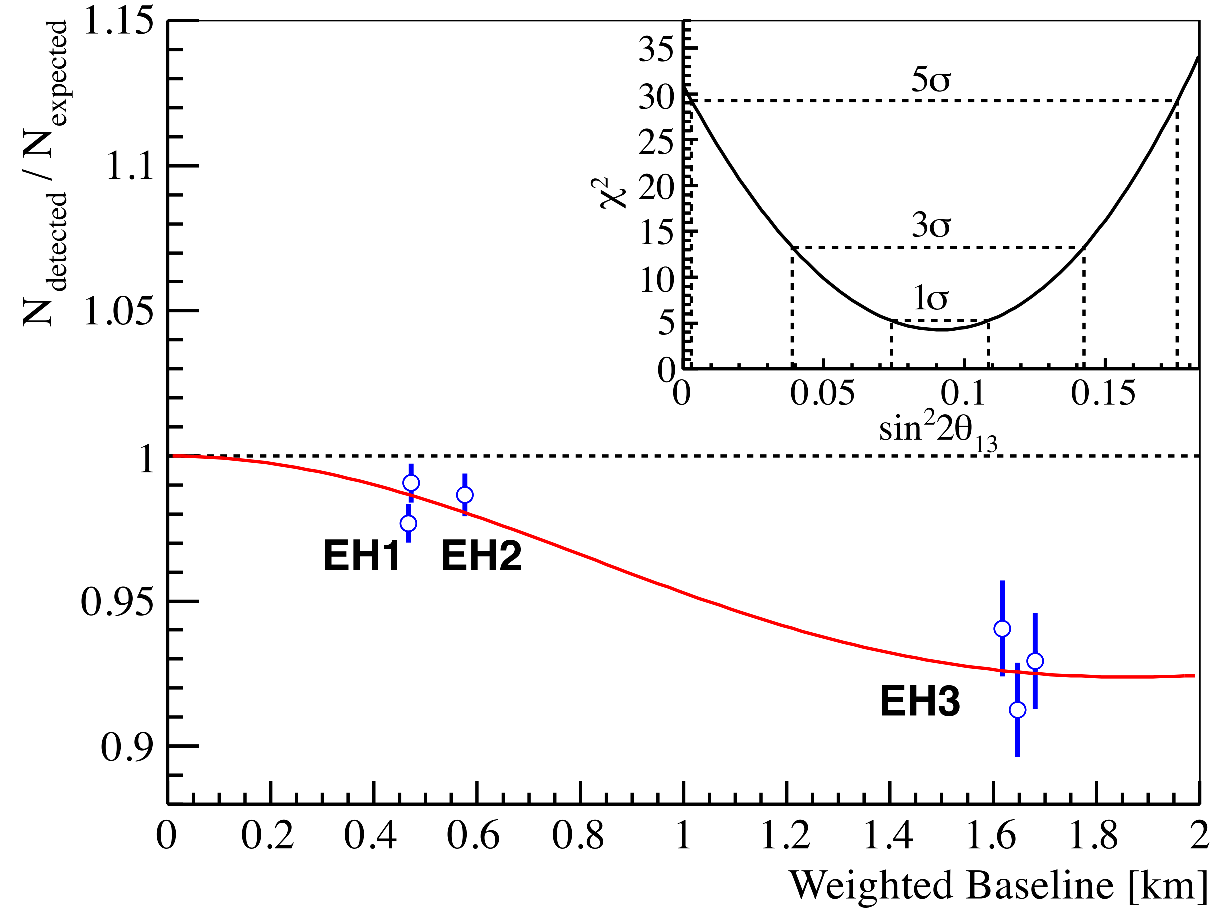

FIG. 4. Ratio of measured versus expected signal in each detector, assuming no oscillation. The error bar is the uncorrelated uncertainty of each AD, including statistical, detector-related, and background-related uncertainties. The expected signal is corrected with the best-fit normalization parameter. Reactor and survey data were used to compute the flux-weighted average baselines. The oscillation survival probability at the best-fit value is given by the smooth curve. The AD4 and AD6 data points are displaced by -30 and +30 m for visual clarity. The χ^2 versus $\sin^2 2\theta_{13}$ is shown in the inset.

$\sin^2 2\theta_{13} = 0.092 \pm 0.016(\text{stat}) \pm 0.005(\text{syst})$ in a three-neutrino framework.

[29] The survival probability used in the χ^2 was $P_{sur} = 1 - \sin^2 2\theta_{13} \sin^2(1.267\Delta m^2_{31} L/E) - \cos^4 \theta_{13} \sin^2 2\theta_{12} \sin^2(1.267\Delta m^2_{21} L/E)$ where, $\Delta m^2_{31} = 2.32 \times 10^{-3}\text{eV}^2$, $\sin^2 2\theta_{12} = 0.861^{+0.026}_{-0.022}$, and $\Delta m^2_{21} = 7.59^{+0.20}_{-0.21} \times 10^{-5}\text{eV}^2$. The uncertainty in Δm^2_{31} [30] has not been included in the fit. The fit $\sin^2 2\theta_{13}$ will change by +0.0007 and -0.0004 when Δm^2_{31} changes by one standard deviation.

Neutrino-Oszillationen Gesamtschau

$$U = \begin{pmatrix} 1 & 0 & 0 \\ 0 & \cos\theta_{23} & \sin\theta_{23} \\ 0 & -\sin\theta_{23} & \cos\theta_{23} \end{pmatrix} \cdot \begin{pmatrix} \cos\theta_{13} & 0 & \sin\theta_{13}e^{-i\delta} \\ 0 & 1 & 0 \\ -\sin\theta_{13}e^{-i\delta} & 0 & \cos\theta_{13} \end{pmatrix} \cdot \begin{pmatrix} \cos\theta_{12} & \sin\theta_{12} & 0 \\ -\sin\theta_{12} & \cos\theta_{12} & 0 \\ 0 & 0 & 1 \end{pmatrix}$$

δ: CP-Phase

2. & 3. Generation	1. & 3. Generation	1. & 2. Generation
atmosphärische ν´s	Reaktorexperimente	solare Neutrinos
long baseline Beschleuniger	long baseline Beschleuniger	Reaktorexperimente
ν_μ - X ν_μ - ν_τ	$\bar{\nu}_e$ – X ν_μ - ν_e	ν_e - X $\bar{\nu}_e$ – X



$\Delta m_{23}^2 = 2.3 \times 10^{-3}$ eV²	$\Delta m_{13}^2 = 2.3 \times 10^{-3}$ eV²	$\Delta m_{12}^2 = 7.9 \times 10^{-5}$ eV²
$\theta_{23} = (45 \pm 4)°$ (maximal)	$\theta_{13} < 15°$ (sehr klein)	$\theta_{23} = (33.7 \pm 1.3)°$ (groß)

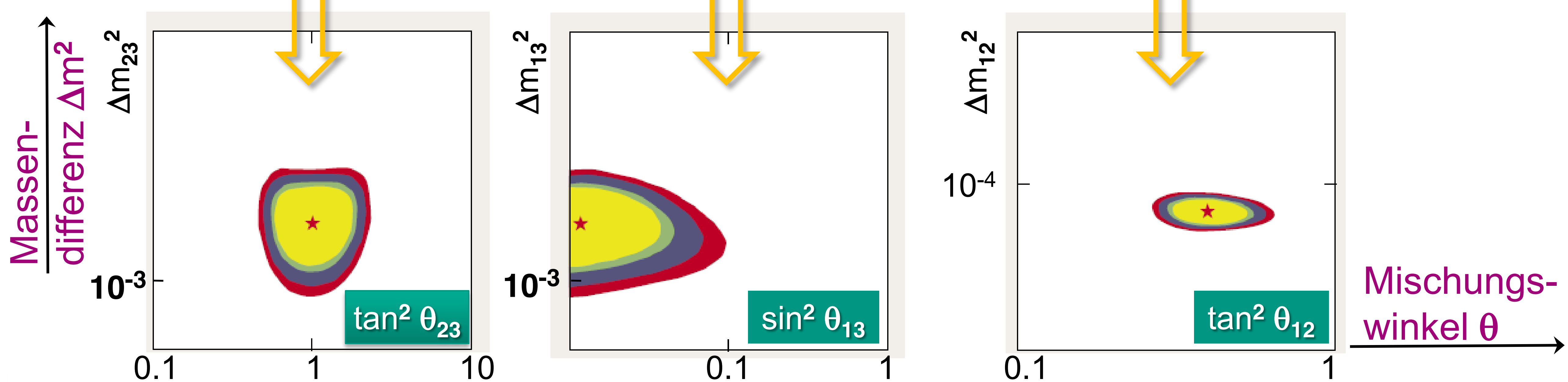

Neutrino-Oszillationen Gesamtschau

$$U = \begin{pmatrix} 1 & 0 & 0 \\ 0 & \cos\theta_{23} & \sin\theta_{23} \\ 0 & -\sin\theta_{23} & \cos\theta_{23} \end{pmatrix} \cdot \begin{pmatrix} \cos\theta_{13} & 0 & \sin\theta_{13} e^{-i\delta} \\ 0 & 1 & 0 \\ -\sin\theta_{13} e^{-i\delta} & 0 & \cos\theta_{13} \end{pmatrix} \cdot \begin{pmatrix} \cos\theta_{12} & \sin\theta_{12} & 0 \\ -\sin\theta_{12} & \cos\theta_{12} & 0 \\ 0 & 0 & 1 \end{pmatrix}$$

δ: CP-Phase

2. & 3. Generation	1. & 3. Generation	1. & 2. Generation
atmosphärische ν´s	Reaktorexperimente	solare Neutrinos
long baseline Beschleuniger	long baseline Beschleuniger	Reaktorexperimente
ν_μ - x ν_μ - ν_τ	$\bar{\nu}_e$ – x ν_μ - ν_e	ν_e - x $\bar{\nu}_e$ – x
		
$\Delta m_{23}^2 = 2.3 \times 10^{-3}\ eV^2$	$\Delta m_{13}^2 = 2.3 \times 10^{-3}\ eV^2$	$\Delta m_{12}^2 = 7.9 \times 10^{-5}\ eV^2$
$\theta_{23} = (45 \pm 4)°$ (maximal)	$\theta_{13} < 15°$ (sehr klein)	$\theta_{23} = (33.7 \pm 1.3)°$ (groß)

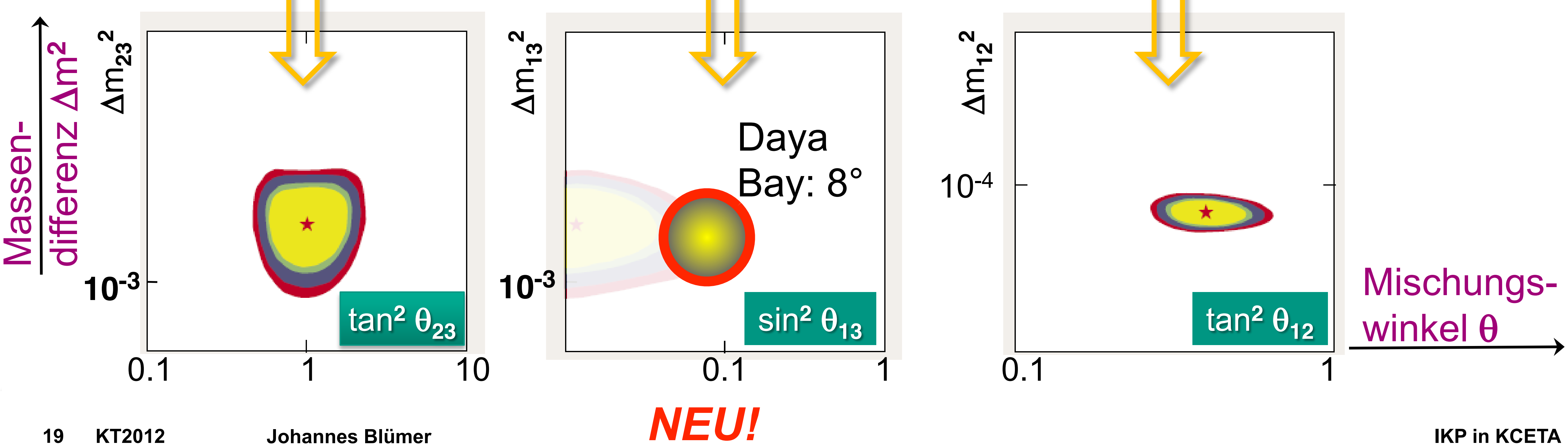

Die absolute Neutrinomasse

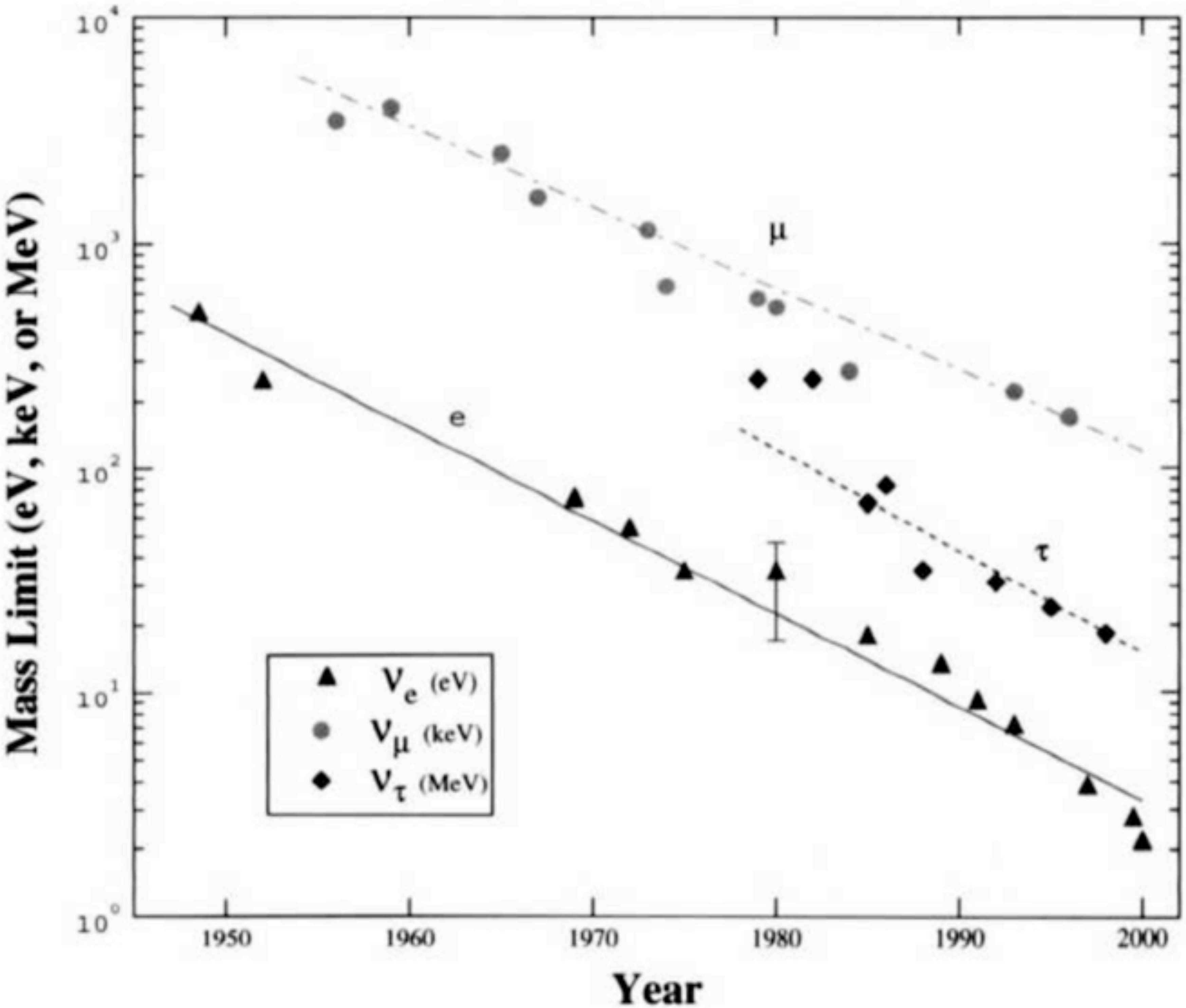

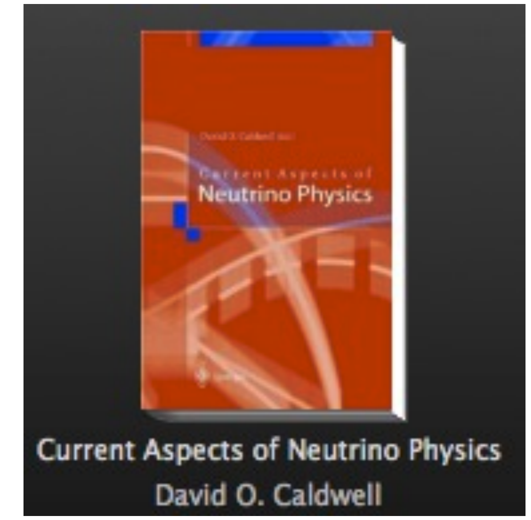

Fig. 3.1. History of direct neutrino mass measurements. *Points without error bars* represent upper limits on the mass values, while the *one point with error bar* represents a nonzero mass result, ruled out by subsequent measurements

Die absolute Neutrinomasse

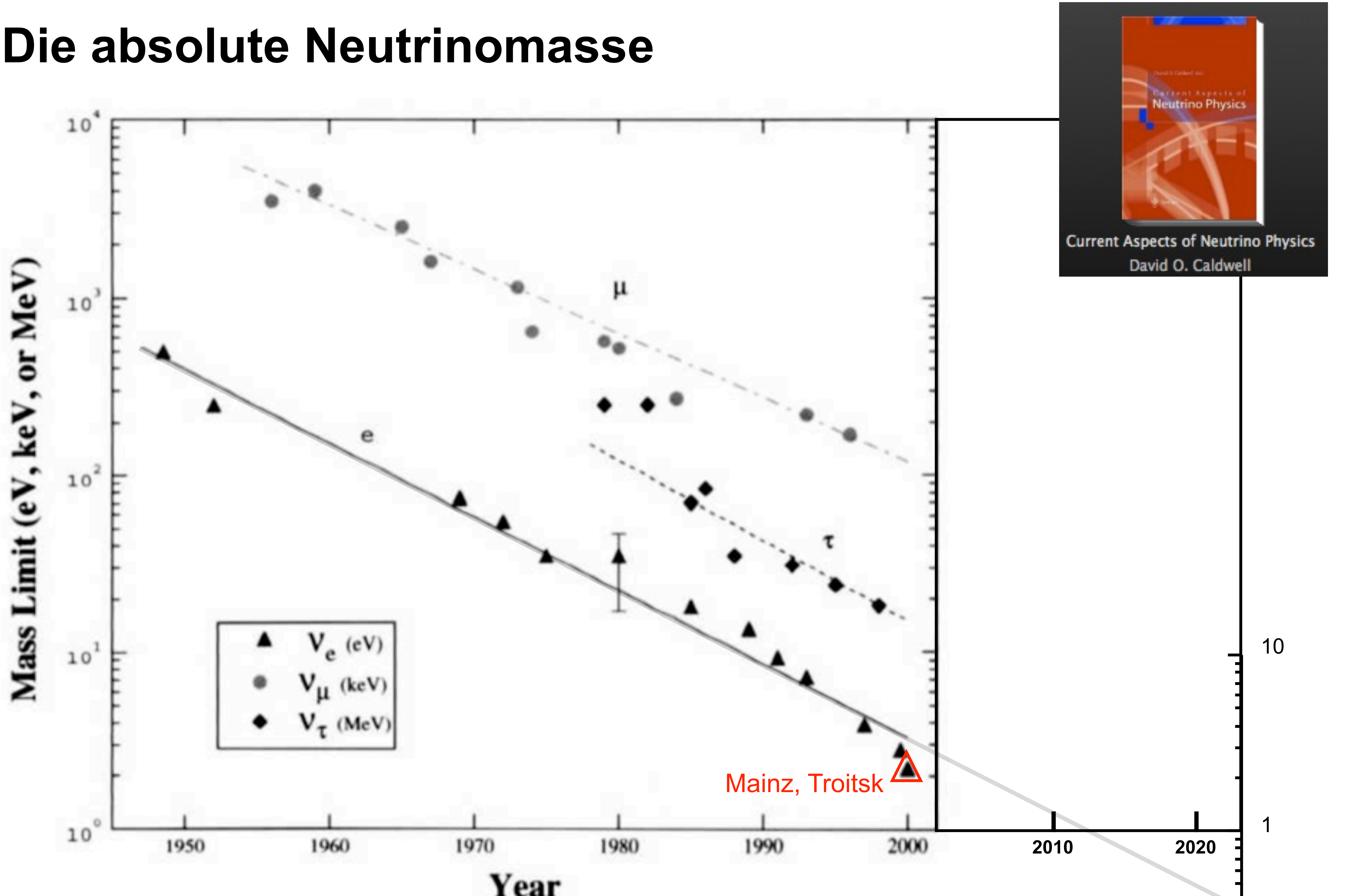

Fig. 3.1. History of direct neutrino mass measurements. *Points without error bars* represent upper limits on the mass values, while the *one point with error bar* represents a nonzero mass result, ruled out by subsequent measurements

Methodenübersicht

- Neutrino-Oszillationen
  - sensitiv nur auf Massendifferenzen^2
- Kinematische ("direkte") Methoden
  - Massenbilanz bei Zerfällen und/oder Reaktionen mit Neutrinos im Endzustand; Beispiel Tritiumzerfall/KATRIN
- Flugzeitmessungen
  - $m_\nu \leq 2$ eV erfordert sehr lange Flugstrecken; Untersuchung des Neutrinopulses von einer (galaktischen) Supernova, z.B. SN1987a
- Neutrinoloser Doppel-Beta-Zerfall ("0νßß")
  - erfordert Majorana-Natur des Neutrinos und Kenntnis nuklearer Matrixelemente...; HD-Moskau, GERDA...
- kosmologische Ableitungen
  - Neutrinos sind die häufigsten massiven Teilchen im Universum, Einfluss auf Massenbilanz (klein) und Strukturbildung (gross)

Methodenübersicht

[Drexlin]

Kinematik ß-Zerfall
absolute ν-Masse: m_ν

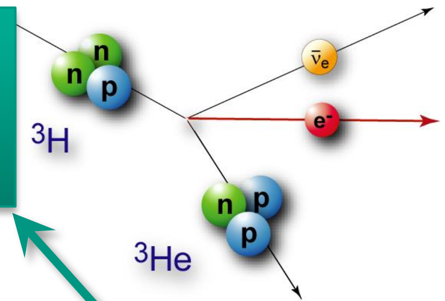

modellunabhängig
Status: $m_\nu < 2.3$ eV
Potenzial: $m_\nu = 200$ meV
KATRIN, (MARE)

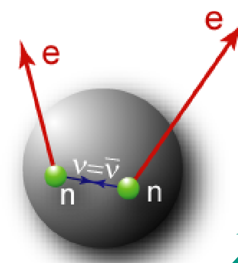

Suche nach 0νßß
eff. Majoranamasse $m_{ßß}$

modellabhängig (CP)
Status: $m_{ßß} < 0.35$ eV, Evidenz?
Potenzial: $m_{ßß} = 20\text{-}50$ meV
GERDA, EXO, CUORE

Neutrinomassen-
experimentelle Techniken

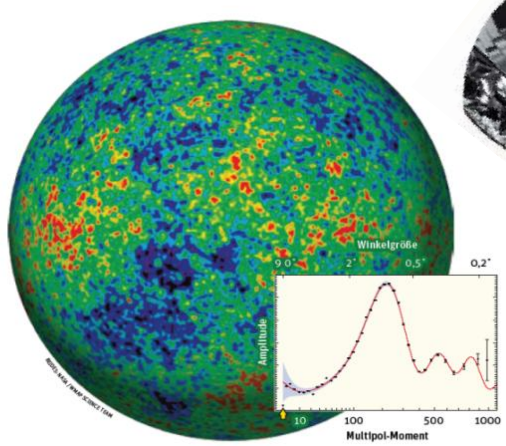

Kosmologie
Summe Σm_i, HDM Ω_ν

modellabhängig (Multiparameter)
Status: $\Sigma m_i < 0.6 - 2$ eV
Potenzial: $\Sigma m_i = 20\text{-}50$ meV
Planck, Gravitationslinseneffekte